Università degli Studi del Piemonte Orientale
"Amedeo Avogadro"

Dottorato di Ricerca in Medicina Molecolare

Development of new molecular markers in immunohematology and oncology

Circulating $CD4^+CD25^+$ and liver-infiltrating $Foxp3^+$ cells as new lymphocyte markers in chronic HCV-associated liver disease

*****

Phenotypical and functional markers in monitoring *ex vivo* expansion of clinical grade Cytokine-Induced Killers cells (CIK)

*****

Nectin like-5 overexpression correlates with malignant phenotype in cutaneous melanoma

Tesi del dr. Alfredo Amoroso

Anno Accademico 2013-2014

SUMMARY

Preface

Development of new molecular markers in immunohematology and oncology

The advances in molecular medicine lead continuously to the discovery of new targets for new possible therapeutic approaches. At the same time the possibility and the need for more efficient biological markers is increased, as well as the necessity of new functional tests or diagnostic algorithms that could be able to optimize monitoring and follow-up of diseases, or obtain an earlier diagnosis.

The works presented here, though focusing on different topics, aim to shed new light on the biological role of newly identified cell subsets and molecules, and their importance as phenotypical and functional markers in human immunohematology and oncology.

The progresses obtained in the field of cellular immunology, and in the definition of specific T cell subsets in particular, contributed to increase our knowledge on the pathogenesis of several diseases which recognize an immunological trigger, as well as on the mechanisms that regulate the omeostasis of cancer cells. These discoveries have allowed the development of new, more efficient drugs, if compared to traditional standard therapies. The study of cellular protagonists of innate and adaptive immunity, moreover, led to the acquisition of new keys to obtain a wider overview of some diseases where the immune system activation acts as a balance between two possible evolutions: such is the case, for example, of HCV-related hepatitis. The prosecution of these studies holds the promise to lead to new information for predicting the natural history of the disease, and to the elaboration of new laboratory-clinical indexes for its monitoring.

The study of growth and proliferation dynamics of Cytokine-Induced Killer cells (CIK) is nowadays important for the assessment of the functionality of cells destined to clinical use, in order to obtain safer and more efficient products. At the same time, the development of new biological markers and functional tests which can be able to provide more information about viability, functionality and duration of infused cells is of great interest.

In clinical oncology, a great effort is being made in order to discover efficient biological markers able to early detect the occurring of a malignant disease. Such biological markers would, for instance, be of great support in the early diagnosis of malignant melanoma, the most dangerous neoplasia of skin. The omeostasis and the pathophysiology of normal melanocytes, as well as malignant melanocytes have currently being dissected in order to achieve this goal.

The data collected in the present studies are a result of independent research, and no conflict of interest exists.

1. Circulating $CD4^+CD25^+$ and liver infiltrating $Foxp3^+$ cells as new markers in chronic HCV-associated liver disease

1.1 Introduction

Hepatitis C virus (HCV)-associated chronic liver disease is a chronic liver inflammation where immune system is unable to efficiently clear the viral infection. Although viral factors are certainly involved, several pathophysiological alterations involving the host immune system have also been suggested to take part in the complex pathogenesis of the disease. It is now well known that a strong early cellular response elicited by effector $CD4^+$ and $CD8^+$ T cells could in some cases be able to clear the virus and solve the infection. However, in most cases the infection becomes chronic. Several humoural and cellular regulatory mechanisms has been claimed to be involved in such phenomenon. One possibility is that the naturally tolerogenic liver microenvironment is responsible for an inappropriate biochemical support for an efficient viral clearance, therefore leading to the selection of lymphocyte subsets different from Th1-oriented effector cells (1, 2). Understanding the role of all the actors of the immune system is therefore crucial for reaching the goal to finding an effective therapy. In line with this concept, the study of new markers of cell-mediated immunity is of great interest.

Previous studies have raised the possibility of an involvement of T regulatory cells (Tregs) in the natural history of a chronic liver inflammation (3). In fact, in HCV-related chronic hepatitis, HCV-specific $CD4^+$ T cells displaying a regulatory phenotype have been identified, and the percentages of peripheral blood Tregs have been correlated to the circulating viral load (4). For these reasons, Tregs have

been thought to be involved in the establishment of a chronic hepatitis and in the defective virus clearance ability of effector cells. However, despite clones of HCV-specific T regulatory cells have been proved to develop during infection and to suppress the anti-viral cytotoxic $CD8^+$ cell response, the real contribution of this lymphocyte subset to the pathogenesis of HCV chronic infection still remains uncertain (5).

1.2 Scientific Background

Immune system in HCV infection. Hepatitis C virus frequently elicits only mild immune responses so that it can often establish a chronic infection where HCV antigens persist and continue to stimulate the immune system. Antigen persistence then leads to profound changes in the infected host's immune responsiveness, and eventually contributes to the pathology of chronic hepatitis. Along with the natural history of chronic hepatitis, the immune system undergoes several changes concerning innate immunity (interferons, natural killer cells), adaptive immune responses (immunoglobulins, T cells), and mechanisms of immune regulation (regulatory T cells). In general, a strong anti-HCV immune response is frequently associated with acute severe tissue damage. In chronic hepatitis C, however, the effector arms of the immune system either become refractory to activation or take over regulatory functions. Taken together these changes in immunity may lead to persistent liver damage and cirrhosis. Consequently, effector arms of the immune system play a pivotal role in triggering the mechanisms of inflammation, necrosis and progression to cirrhosis. Thus, avoiding a strong, sustained antiviral immune response with initial tissue damage, takes the infected host to virus-triggered immunopathology, which ultimately leads to cirrhosis and liver cancer (6).

The most conclusive experiments to suggest an important role for T cells in protective immunity against HCV stem from chimpanzee experiments: depletion of $CD8^+$ T cells in animals, which had recovered from previous hepatitis C, resulted in prolonged viraemia, and viral

clearance was correlated to recovery of HCV-specific $CD8^+$ T cells (7). Likewise, depletion of $CD4^+$ T cells resulted in abrogation of a previously protective immune response (8). In acute hepatitis C, strong HCV-specific CTL (9, 10) and Th1 type $CD4^+$ T helper cell responses have consistently been reported to be closely associated with a self-limited course of HCV infection. Moreover, several groups have reported an inverse relationship between the strength of the CTL response and HCV viral loads, further suggesting that in principle it is possible for cellular immunity to control HCV infection (11). A substantial proportion of individuals who ultimately develop chronic hepatitis C also generates HCV-specific $CD4^+$ and $CD8^+$ T cell responses during the early acute phase of infection and may transiently gain some control over HCV (12). However, early T cell responses decline to almost undetectable levels later on, and initial control over HCV replication is lost, though HCV-specific $CD4^+$ and $CD8^+$ T cells can be found enriched within the liver parenchyma (13, 14). Thus, chronic hepatitis C is characterized by a progressive functional exhaustion of HCV-specific $CD4^+$ and $CD8^+$ T cells (15). Exhausted T cells exhibit characteristic abnormalities: they show increased expression of inhibitory receptors, such as programmed death-1 (PD-1), cytotoxic T lymphocyte antigen 4 (CTLA-4), T cell immunoglobulin and mucin domain-containing molecule 3, corresponding to up-regulated expression of their cognate ligands in the liver (16-18). Conversely, functional recovery of HCV-specific T cells can be achieved experimentally by the combined blockade of CTLA-4 and PD-1 signalling. Thus, prolonged exposure appears to be the mechanism that leads to T cell dysfunction in chronic hepatitis C (19).
In the last years, increasing evidences have shown how other important actors play a role in HCV-related chronic liver disease. Among these, regulatory T cells.

Regulatory T cells. Regulatory T cells play an important role in maintaining self-tolerance through their inhibitory functions on effector T cells, preventing the development of autoimmunity (20). While thymic deletion of self-reactive T cells provides a first line mechanism of central tolerance, Tregs represent a peripheral system to maintain self-tolerance and prevent over-exuberant immune responses; thanks to

this second mechanism, self-reactive T cells escaped to intrathymic selection are controlled at the periphery; moreover, peripheral regulation is able to control excessive effector T cell responses against exogenous antigens, when their activation becomes deleterious, or to prevent the functional exhaustion of effector cells, thus granting a long term immunity (21). Mice with mutations in a critical Treg gene (Foxp3) develop a fatal lymphoproliferative syndrome characterized by multi-organ inflammation (22). Immunologically, Tregs comprise a subset of $CD4^+$ lymphocytes that suppresses activation, proliferation, and effector responses of both innate and adaptive immune cells. Functional Tregs also express the interleukin-2 (IL-2) receptor α-chain (CD25), although activated conventional T cells also transiently express CD25. Like conventional T cells, Tregs require T cell receptor (TCR) stimulation and costimulation for activation (23). Natural Tregs (nTregs) are a Treg subset derived centrally in the thymus and represent about 1-3% of all $CD4^+$ T cells. They express surface markers of activated, antigen primed, memory T cells: CD25, CD45RBlow, CD62L, CD103, cytotoxic T lymphocyte antigen-4 (CTLA-4), and glucocorticoid-induced tumor necrosis factor receptor (GITR) (21). Regulatory T cells might act multi-directionally by preventing migration of effector cells, or inhibiting their cooperation with antigen-presenting cells (APC) and thus inducing anergy. They are also capable of killing effector cells or APCs via direct cell-cell contact. Treg cells require T-cell receptor (TCR) stimulation to exert suppression, however, once activated they mediate inhibitory effects without antigen specificity. IL-2 is also specifically required for the Treg maintenance and expansion (21).

Apart from natural Treg cells originating in the thymus (nTreg), other Treg subsets can be induced from peripheral naïve T $CD4^+CD25^{neg}$ cells (Peripherally-induced Tregs, adaptive [aTregs], or Induced Tregs [iTregs]). These subsets can arise under specific influences of the microenvironment, and acquire different phenotypical features and functional properties. The so called Tr1 cells develop under the control of IL-10-conditioned DCs: they are marked by a high IL-10 production; this subtype does not seem to express FOXP3. Another subset is induced from peripheral unprimed $CD4^+$ T cells under the influence of TGF-β and is phenotypically indistinguishable from thymus-derived

nTregs, including the expression of FOXP3 protein (24, 25). Circulating and tissue iTreg numbers depend on anatomic location as well as specific inflammatory environmental conditions. Abbas and other authors recently published recommendations for Treg nomenclature (26). Many efforts are currently being made in order to use Tregs as adoptive T cell immunotherapy; however, clinical implementation of protocols employing Treg cellular products is still challenging (27).

Regulatory T cells in HBV and HCV infection. Since the first report on the presence of regulatory T cells in the liver during viral infections by MacDonald and coworkers in 2002 (28), the scientific debate had focused on the question whether the action of Tregs in the context of a chronic infection is useful as it limits the extent of tissue damage or rather detrimental because of its negative regulation of the effector cell response. This issue still remains a matter of controversies. Many works have demonstrated how Treg cells are able to impair the response of effector cells to HCV antigens (29-31). In particular, they have been shown to suppress IFN-γ secretion by $CD4^+$ and $CD8^+$ T cells and inhibit their proliferation in response to antigenic stimuli. Recently $CD8^+$ T cells have been reported in the livers of patients with chronic hepatitis C which were considered to represent $CD8^+$ regulatory T cells, because they secrete IL-10 and suppress in vitro proliferation of liver-derived T cells (32). On the other hand, Tregs have been proved to limit the activation-induced cell exhaustion and apoptosis of effector cells, thus granting the survival of a memory pool and a long lasting immunity (33-35). Of note, intrahepatic regulatory T cells in chronic hepatitis C also produced substantial amounts of IL-8, and isolated Tregs as well as Treg clones activated fibrogenic genes of hepatic stellate cells in vitro (36). High intrahepatic IL-8 mRNA levels in chronic hepatitis C have been linked with progression of fibrosis and $CD4^+$ Tregs are enriched in the liver (37-41).

Future developments. In order to acquire more knowledge on this issue, further studies should aim to correlate the presence, the phenotypical features and the functional ability of intrahepatic Tregs to the clinical, long term evolution of HCV infection. While monitoring of the clinical

evolution of HCV infection can be easily achieved by routine follow-up including serum transaminase levels, viremia load and ultra-sound scan, intra-hepatic detection and characterization of Tregs would require the establishment of a defined liver biopsy schedule, during long term follow-up, and the consequent execution of immunohistochemical studies in order to fully characterize the cellular populations present within the liver infiltrates; in this context, tridimensional stereology calculations from histological data would represent a fascinating source of further information from ex-vivo material (42, 43).

1.3 Study design

The aim of the present study was to acquire further information on the clinical impact of $CD4^+$ T cells with a regulatory phenotype during the evolution of a chronic liver disease caused by HCV infection. Both peripheral blood and intrahepatic regulatory T cells were investigated, the former by flow cytometry analysis of whole blood samples from HCV^+ patients, the latter by immunohistochemical staining of liver biopsy samples from the same patients. Along with circulating Tregs, the presence of other T cell subsets was assessed, in particular $CD4^+$CD25low or $CD25^{neg}$ T cells and $CD8^+$ T cells. In order to explore the clinical state of the disease, serum transaminase levels, viremia load, ultra-sound and conventional histology score were evaluated and correlated to immunological data.

1.4 Materials and methods

Patients. Thirty patients with HCV-related chronic hepatitis were recruited at the Department of Internal Medicine of P.O. ‘G. Rodolico’, Azienda Ospedaliero-Universitaria ‘Policlinico - Vittorio Emanuele’, Catania, Italy. They were followed-up by clinical examination, measurement of transaminase plasma levels and circulating viral load,

and ultrasound exploration of the liver. They were also subjected to liver biopsies to assess the hepatitis activity and the fibrosis stage.
The patients included 12 males and 18 females, aged between 39 and 71 years. The modality of infection was in all cases considered as community acquired or undetermined. The HCV genotype was 1b in all patients. Only 2 patients were already receiving therapy at the time of analysis (Rebetol 1200 mg and PegIntron 135 mg). The controls comprised healthy volunteers, 13 males and 7 females, aged between 28 and 61 years. The study was approved by the local ethics committee.
Sample and tissue collection. After having obtained informed consent from all patients, PB specimens were drawn from the patients and control subjects and collected in heparin collection tubes. Needle liver biopsies were obtained percutaneously from the patients.

Clinical laboratory analysis. Serum transaminase levels were measured by using a Modular Analytics instrument (Roche, Diagnostics, Indianapolis, IN, USA).

Histological evaluation. Liver specimens were fixed in 10% neutral-buffered formalin and processed for embedding in paraffin wax. Sections of tissue were stained with hematoxylin and eosin for standard light microscopic evaluation using standard methods. The biopsies were classified according to the Sheuer score (portal activity/lobular activity and fibrosis, from 0 to 4) by an expert pathologist.

Immunohistochemical analysis. Tissue sections (5 μm) were microwave-heated for 15 min in 10 mM citrate buffer (pH 6.0) (Millipore, Billerica, MA, USA). They were then treated with 1% hydrogen peroxide for 15 min and subsequently blocked with pre-diluted normal goat serum (Santa Cruz Biotechnology Inc., Santa Cruz, CA, USA) for 20 min at room temperature. Sections were then incubated with anti-Foxp3 antibodies (dilution 1:100, sc-80792; Santa Cruz Biotechnology Inc.) and stained with the streptavidin-biotin-peroxidase complex system (ImmunoCruz™ Staining System; Santa Cruz Biotechnology Inc.). Finally, the sections were counterstained with Mayer's hematoxylin. Slides were dehydrated, mounted and observed by conventional light microscopy. Negative control staining

was performed by substituting the primary antibody with non-immune serum.

Flow cytometry analysis. Whole blood samples were tested for leukocytes surface antigens by using FITC-conjugated CD4, PE-conjugated CD8, and PECy5-conjugated CD25 monoclonal antibodies (mAb) (Becton-Dickinson, Franklin Lakes, NJ, USA). The cells were then permeabilized with the Foxp3 Buffer Set (eBioscience, San Diego, CA, USA), stained with APC-conjugated anti-Foxp3 mAb (Becton-Dickinson), and fixed in PBS containing 1% of paraformaldehyde. Control stainings were performed with the appropriate isotype matched antibody.
For detection of IFN-γ producing cells, 500 μl of whole blood were mixed with 500 μl of RPMI-1640 medium with glutamine and stimulated with 25 ng/ml of phorbol 12-myristate, 13-acetate (PMA; Sigma Chemical Co., St. Louis, MO, USA) and 1 μg/ml of ionomycin (Sigma) in the presence of brefeldin (Becton-Dickinson). The cells were then incubated in 15 ml tubes at 37˚C in 5% CO2, humidified atmosphere for 4 hours. After incubation, surface and intracellular staining were performed as indicated above, by using the anti-CD4 mAb and anti-Foxp3 mAb plus a PE-conjugated anti-IFN-γ mAb (Becton-Dickinson); these cells were not stained for CD25, since preliminary experiments showed a substantial down-modulation of this marker upon treatment with PMA + ionomycin. The samples were analysed in a FACSCalibur cytometer (Becton-Dickinson).

Statistical analysis. The percentages of T cell subsets in the examined groups were expressed as median and interquartile ranges (IR). The statistical significance was assessed by the Mann-Whitney U test. Differences were considered to be statistically significant at a level of $p<0.05$.

1.5 Results

At the histological evaluation executed by an expert pathologist, the patients displayed a grading (portal activity vs lobular activity) ranging from 1/0 to 3/2; fibrosis was classified from stage 1 to 3.

Sheuer's score	No. of specimens (n=30)	Foxp3$^+$	Foxp3$^-$	p[1]
1/0/1	2	0	2	
2/1/1	1	0	1	
2/1/2	3	1	2	
2/2/1	4	0	4	0.72
2/2/2	3	3	0	
3/1/2	4	2	2	
3/2/2	8	3	5	
3/2/3	5	2	3	
[1]Yates' chi square test.				

Table 1. Association of Foxp3 expression with Sheuer's score in HCV-affected liver sections.

The immunohistochemical analysis for Foxp3, detected positive cells in 11 out of 30 patients (Table I), and showed that Foxp3$^+$ cells were found among the lymphocytes infiltrating the portal area (Fig. 1).

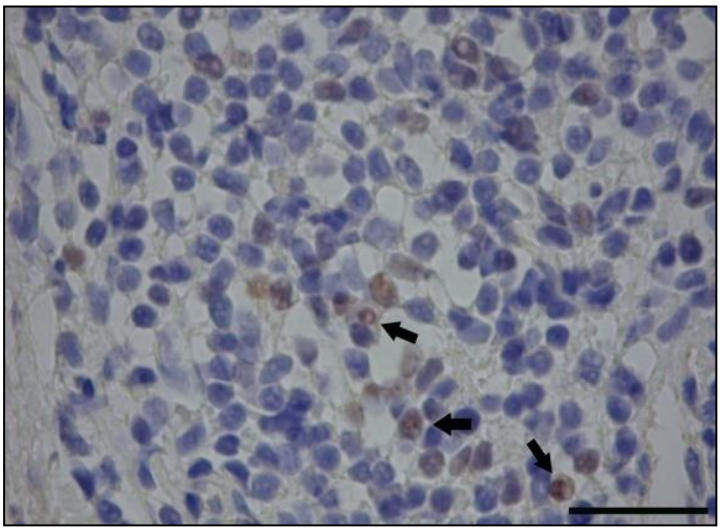

Figure 1. Representative micrograph of liver section from a HCV affected patient. Some lymphocytes are immunolabelled for Foxp3 (arrows) (bar: 60 µm).

Transaminase levels were elevated in most patients: 29 and 19 patients for alanine transaminase (ALT) and aspartate aminotransferase (AST), respectively. The mean ALT serum level was 97.27±32.09 U/l in $Foxp3^{+}$ patients vs 127±33.22 in $Foxp3^{neg}$ patients; the mean AST serum level was 56.73±28.09 U/l in $Foxp3^{+}$ patients vs 76.21±32.21 in $Foxp3^{neg}$ patients. Such a difference between the mean values of $Foxp3^{+}$ and $Foxp3^{neg}$ patients resulted in a statistical significance for ALT (p=0.03) (Table II).

	Foxp3⁻ (n=19)	***Foxp3⁺ (n=11)***
ALT (U/L)		
mean value (SD)	127 (33.22)	97.27 (32.09)
median (IQR)	128 (106-156)	102 (74-119)
p		**0.03**
AST (U/L)		
mean value (SD)	76.21 (32.21)	56.73 (28.09)
median (IQR)	72 (53-102)	57 (27-69)
p		0.08

Table 2: Mean ALT and AST serum concentrations in the patients subgrouped by Foxp3 liver immunohistochemistry. The difference between patients with Foxp3+ and Foxp3- histology is statistically significant for ALT (p= 0,03).

Flow cytometry analysis of the peripheral blood samples showed a relative increase in the total amount of lymphocytes in the patients compared to the controls; the median percentage of circulating lymphocytes was 27.85% (IR 25.82-30.91%) in the patients and 25.02% (IR 17.08-28.54%) in the controls (p=0.02). Within the lymphocyte population, the median percentage of T helper $CD4^{+}$ cells was 44.20% (IR 40.06-49.87%) in the patients and 37.20% (IR 31.41-42.52%) in the controls (p=0.0002); the median percentage of $CD8^{+}$ T cells was 38.63% (IR 34.70-39.77%) in the patients and 23.87% (IR 19.45-25.28%) in the controls (p<0.0001). In $CD4^{+}$ lymphocytes, the expression of CD25 distinguished 3 subsets: $CD4+CD25^{neg}$, $CD4^{+}CD25^{low}$ and $CD4^{+}CD25^{high}$. The marker separating the $CD25^{low}$

and $CD25^{high}$ subset was set at 1 logarithmic decade from the $CD25^{neg}/CD25^{low}$ cut-off value (Fig. 2a). Within the $CD4^{+}$ cells, the median percentages of $CD25^{neg}$, $CD25^{low}$, and $CD25^{high}$ cells were 47.13% (IR 42.27-60.58%), 49.59% (IR 38.57-53.84%) and 2.47% (IR 1.67-3.44%) in the patients, and 64.39% (IR 56.71-72.59%), 32.13% (IR 24.45-39.42%), and 3.01% (IR 2.32-3.29%) in the controls, respectively. The proportions of $CD25^{low}$ cells were significantly higher and those of $CD25^{neg}$ cells significantly lower in the patients in comparison to the controls ($p<0.0001$), whereas those of $CD25^{high}$ cells were not different between the 2 groups ($p=0.08$) (Fig. 2b).

Foxp3 staining was positive but at a low intensity in the $CD4^{+}CD25^{high}$ cells only (Fig. 3), and the Foxp3 mean fluorescence in this population was not significantly different between the patients and the controls (21.61±9.39 vs. 20.34±10.21, $p=0.65$). Of note, the proportion of PB $CD4^{+}CD25^{low}$ cells was significantly higher in the patients displaying a positive intrahepatic immunolocalization of $Foxp3^{+}$ cells compared to those displaying a negative one (52.87%, IR 41.80-57.73% vs. 41.26, IR 37.54- 50.24%; $p=0.04$) (Fig. 4). The liver biopsies from the 2 patients receiving therapy were positive for Foxp3. No difference was found in the $CD4^{+}CD25^{high}$ and $CD4^{+}CD25^{neg}$ cell proportions between the patients who were $Foxp3^{+}$ and Foxp3neg at a the immunohistochemical level.

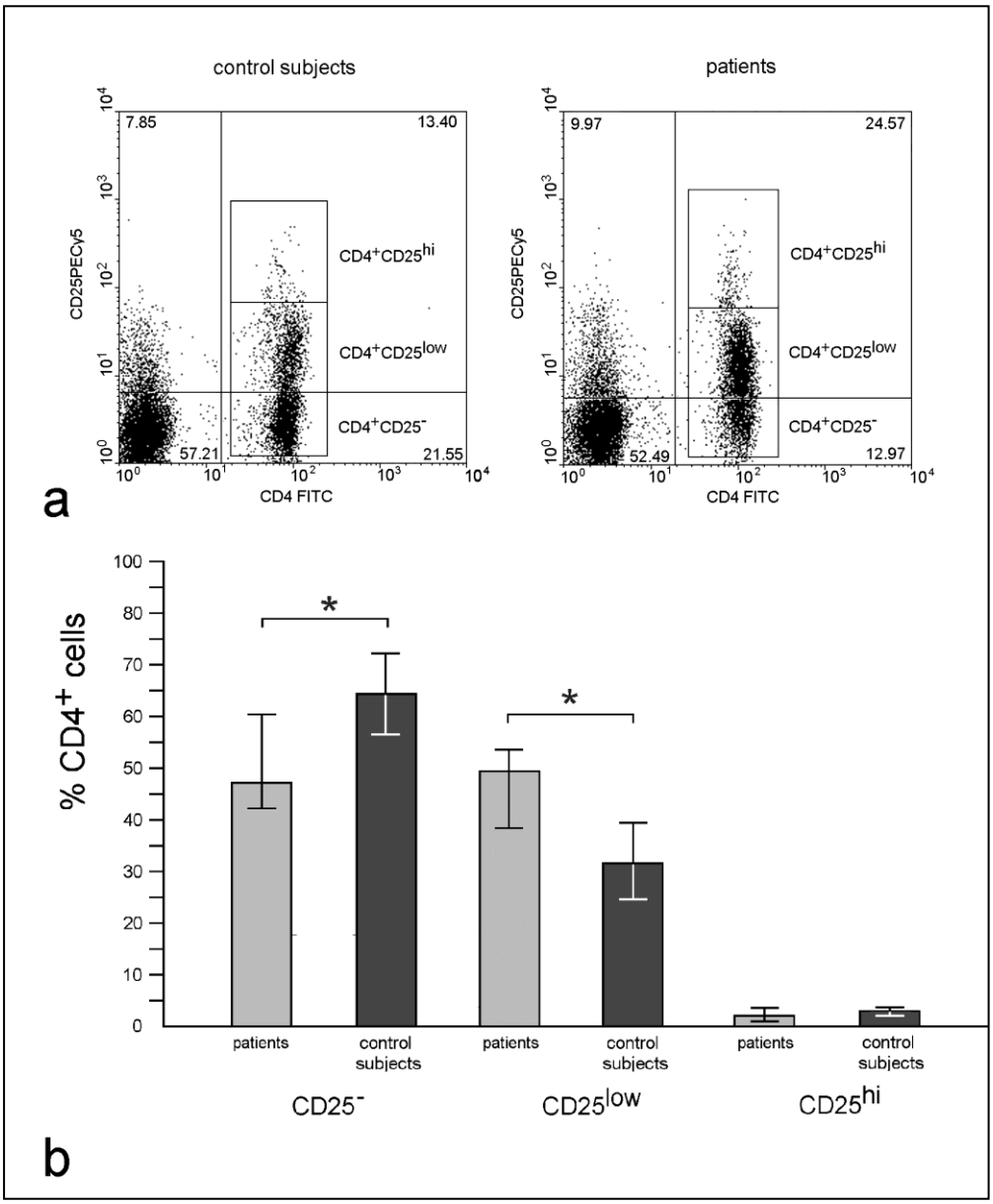

Figure 2. (a) Representative dot plots from peripheral blood. The cytograms show the expression of CD4 and CD25 in the peripheral blood lymphocyte population of healthy controls and patients. **(b) Bar histogram representing the mean percentages of $CD25^{-}$, $CD25^{low}$ and $CD25^{hi}$ cell populations among the $CD4^{+}$ cells in peripheral blood lymphocytes, in patients and controls.** The percentage of $CD4^{+}CD25^{low}$ cells is increased in the patients, compared to controls. $^{a}P<0.0001$.

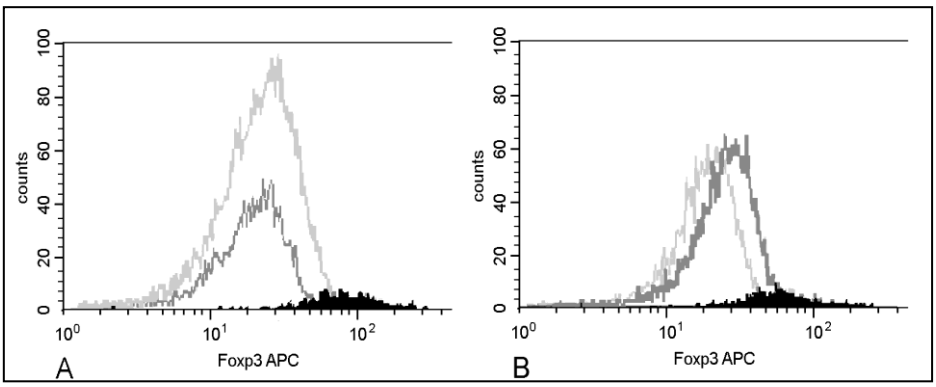

Figure 3. Histograms representing Foxp3 expression intensity among the CD25neg, CD25low (empty histograms) and CD25high (filled histograms) cell populations in controls (A) and patients (B). The CD4+CD25high cells are Foxp3+ at low intensity, while the CD4+CD25neg and the CD4+CD25low cells are Foxp3neg. The fluorescence intensity of the isotype control resulted similar to the intensity of the anti-Foxp3 antibody in the CD4+CD25neg and CD4+CD25low cells (data not shown).

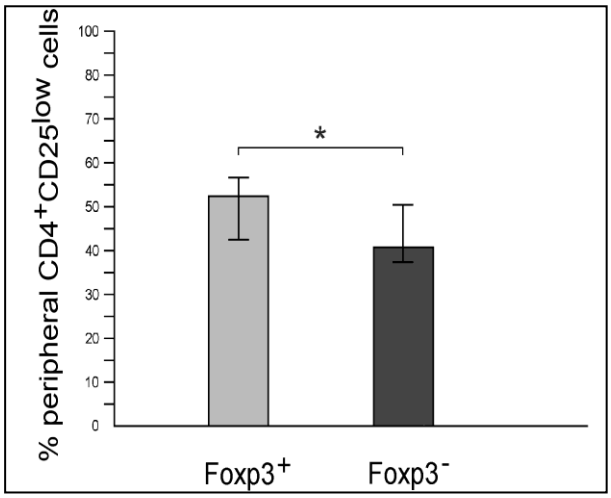

Figure 4. Median percentages of $CD25^{low}$ cells in peripheral $CD4^+$ T cell population in patients subgrouped for liver Foxp3 expression. $^bP<0.05$.

After stimulation with PMA and ionomycin, analysis of IFN-γ expression showed higher median percentages of IFN-γ^+ cells in the patients (34.25%, IR 30.85-39.37%) in comparison to the controls (17.13%, IR 13.91-20.40%) ($p<0.0001$); this difference was significant in both $CD4^+$ (12.61%, IR 10.38-17.42% vs. 4.84%, IR 3.49-7.23%)

and $CD4^{neg}$ (20.65%, IR 18.71-25.02%, vs 10.51%, IR 7.37-14.89%) subpopulations ($p<0.0001$) (Fig. 5a). After in vitro stimulation, the proportion of $Foxp3^+$ cells was still not significantly different between patients and controls: 1.21% (IR 0.15-2.87%) in the control subjects, 1.27% (IR 0.24-3.11%) in patients. As expected, Foxp3 was expressed only in $CD4^+$ cells (data not shown) and double-positive IFN-γ / $Foxp3^+$ cells were substantially absent (Fig. 5b).

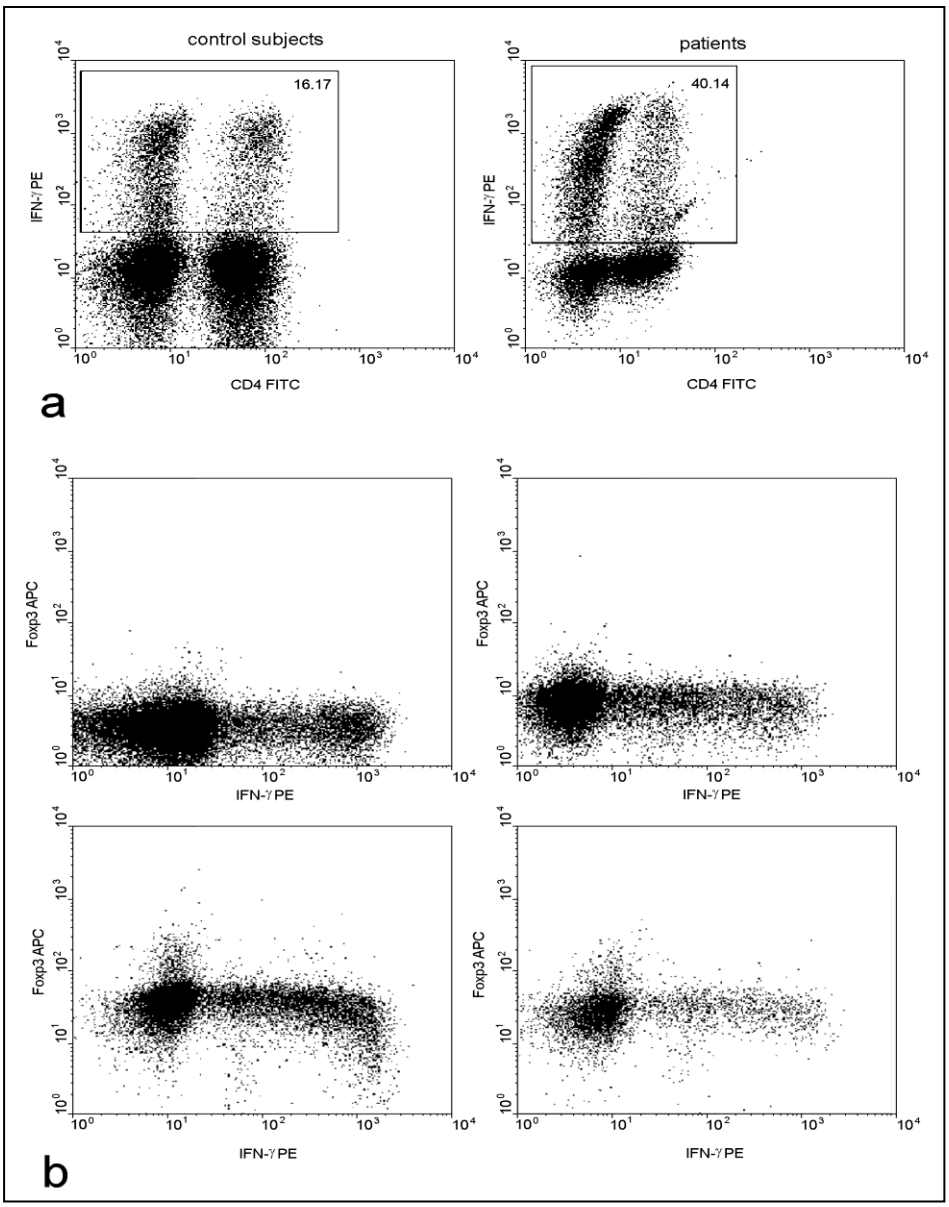

Figure 5. (a) Representative dot plot cytograms showing the expression of CD4 and IFN-γ after stimulation with 25 ng of PMA and 1 µg of ionomycin, in the peripheral blood lymphocyte population, in the healthy controls and in the patients. The percentage of IFN-γ+ cells is increased in the patients, both from the CD4+ and CD4neg subsets. **(b) Representative dot plot cytograms showing the**

expression of IFN-γ and Foxp3 after stimulation with 25 ng of PMA and 1 µg of ionomycin, in the peripheral blood lymphocyte population in the patients. No populations are identifiable showing a double positivity for the two markers.

1.6 Discussion

In HCV-associated chronic liver disease, the immune system is unable to effectively clear the viral infection, despite the activation of humoural and cellular immune responses (44). A number of viral factors are involved in this process, such as the ability of HCV to modify its surface antigens and to exploit different entry mechanisms to infect target cells (45). However, the highly tolerogenic liver microenvironment, rich in TGF-β and other profibrotic factors, may also inhibit an effective viral clearance by favouring the switch to an immune response pattern different from Th1 (46-48). Antiviral $CD4^+$ and $CD8^+$ T cell activity is therefore dampened, and these cells are likely to either switch to an anergyc state or acquire regulatory functions, by producing different cytokine profiles (TGF-β or IL-10) and exhibiting different surface markers, like FOXP3, PD-1 and CTLA-4.

The role played by regulatory T cells in this balance has been discussed in previous studies but not clearly defined. In particular, they have been shown to be able to impair the response of effector cells to HCV antigens and suppress IFN-γ secretion by $CD4^+$ and $CD8^+$ T cells (29-31); on the other hand, other evidences support the concept that Tregs are able to limit the activation-induced cell exhaustion and apoptosis of effector cells, thus granting the survival of a memory pool and a long lasting immunity (33-35). The role of all the alternatively differentiated regulatory lymphocyte subsets is, however, crucial in the final outcome of the disease, and further information are needed to clearly identify their phenotypical and functional markers.

In the present study, we tried to correlate the clinical history of the disease (by routine clinical monitoring) to the immunological activation state in the peripheral blood and within the liver parenchyma. We found that the concentrations of serum transaminases were lower in the patients displaying $Foxp3^+$ cells in the liver inflammatory infiltrates

than in those lacking these cells, though these results reached the statistical significance for ALT transaminase only. Moreover, the proportion of peripheral blood $CD4^{+}CD25^{low}$ cells, comprising the activated-effector compartments of T helper cells, was significantly higher in the same patients.

As expected, we found that the proportions of circulating $CD4^{+}CD25^{low}$ T cells, were increased in the patients compared to the controls. This supports their possible involvement in the anti-viral response. In line with these findings, the proportions of IFN-γ-secreting cells were also increased in the patients, in both $CD4^{+}$ and $CD4^{neg}$ lymphocyte cell subsets, as expected in a viral infection.

By contrast, in our study, the proportions of circulating $CD4^{+}CD25^{high}Foxp3^{+}$ T cells, comprising cells with Treg activity (referred to as natural Tregs), were not significantly different in the patients and the controls. Similar to the results from other studies (49, 50), no double-positive IFN-$\gamma^{+}Foxp3^{+}$ cells were found in our experiments, making it unlikely that $Foxp3^{+}$ cells are simply activated effector cells.

Our findings are in line with the notion that Treg cells help to direct the anti-viral response towards the appropriate exogenous targets, limiting the damage to tissues due to either exaggerated effector responses, or autoreactive responses secondary to molecular mimicry. The notion that Tregs infiltrating the liver are associated to a higher presence of immunocompetent $CD4^{+}$ cells in the peripheral circulation could offer an interesting point of speculation, as this might indicate that natural Tregs could also influence the overall homing network of immune cells. Moreover, as demonstrated by different authors (34, 35), suppression may even prolong the immune response by preventing the massive activation and the consequent exhaustion of effector cells.

Our findings are consistent with the study of Ward et al (51) in the idea that the main effect of Treg presence and activation within the liver parenchyma during HCV infection leads to a relative reduction in liver inflammation while the Treg presence may favour fibrogenesis by the production of TGF-β. However, since the correlation with fibrosis still remains unclear, analysis of the TGF-β distribution pattern in relation to the presence of $Foxp3^{+}$ cells within the liver should be taken into consideration as an important goal in further studies.

It must be underlined that other subsets of Tregs may be involved in the disease, but they have not been evaluated in this study since their detection is elusive (52); these different subsets (indicated as peripherally-induced Tregs), which can be either $CD4^+$ or $CD8^+$, are often Foxp3neg and may differentiate from inappropriately activated naive T cells, such as those activated in the absence of costimulatory signals or in the presence of high levels of TGF-β or IL-10, which are abundant in the liver (53). Alternatively, they may differentiate from exhausted effector lymphocytes.

1.7 Conclusions

In conclusion, it is possible to assume that Treg cells are likely to exert a control on HCV-specific cell-mediated immune response. Such a control, however, would function as a general mechanism to limit tissue damage, and to prevent the exhaustion of effector cells. It is also reasonable, that due to their great heterogeneity and plasticity, some liver-infiltrating T cells, conditioned by the local cytokine milieu, may develop phenotypes which may favour fibrogenesis. Moreover, as a result of an aberrant activation mechanism during HCV-associated chronic inflammation, some HCV-specific T cells displaying a regulatory phenotype, can differentiate in the liver from naïve $CD4^+$ T cells, being able to inappropriately inhibit the anti-viral immune response (4, 52).

More experience is to be acquired in this direction, with special regard to assess new intra-hepatic fibrosis markers that could be able to correlate the entity of fibrosis to the presence, activity and persistence of cellular actors. Therefore, further studies should be designed by recruiting higher number of patients and extending the histological analysis pattern in order to acquire more information on Treg activity within the liver parenchyma. Of note, stereology quantification studies should provide further fascinating source of speculation.

1.8 References

1. Mengshol JA, Golden-Mason L and Rosen HR: *Mechanisms of disease: HCV-induced liver injury*. **Nat Clin Pract Gastroenterol Hepatol**, 2007; 4: 622-634.

2. Racanelli V and Manigold T: *Presentation of HCV antigens to naive CD8+T cells: why the where, when, what and how are important for virus control and infection outcome*. **Clin Immunol**, 2007; 124: 5-12.

3. Cabrera R, Tu Z, et al: *An immunomodulatory role for CD4+CD25+ regulatory T lymphocytes in hepatitis C virus infection*. **Hepatology**, 2004; 40: 1062-1071.

4. Ebinuma H, Nakamoto N, et al: *Identification and in vitro expansion of functional antigen-specific CD25+ FoxP3+ regulatory T cells in hepatitis C virus infection*. **J Virol**, 2008; 82: 5043-5053.

5. Dolganiuc A and Szabo G: *T cells with regulatory activity in hepatitis C virus infection: what we know and what we don't*. **J Leukoc Biol**, 2008; 84: 614-622.

6. Spengler U1, Nischalke HD, et al: *Between Scylla and Charybdis: The role of the human immune system in the pathogenesis of hepatitis C*. **World J Gastroenterol**, 2013; 19(44): 7852-66.

7. Shoukry NH, Grakoui A, et al: *Memory CD8+ T cells are required for protection from persistent hepatitis C virus infection*. **J Exp Med**, 2003; 197: 1645-1655.

8. Grakoui A, Shoukry NH, et al: *HCV persistence and immune evasion in the absence of memory T cell help*. **Science**, 2003; 302(5645): 659-62.

9. Lechner F, Wong DK, et al: *Analysis of successful immune responses in persons infected with hepatitis C virus*. **J Exp Med**, 2000; 191(9):1499-512.

10. Thimme R, Oldach D, et al: *Determinants of viral clearance and persistence during acute hepatitis C virus infection*. **J Exp Med**, 2001; 194(10):1395-406.

11. Koziel MJ, Wong DK, et al: *Hepatitis C virus-specific cytolytic T lymphocyte and T helper cell responses in seronegative persons*. **J Infect Dis**, 1997; 176(4):859-66.

12. Folgori A, Spada E, et al: *Acute Hepatitis C Italian Study Group: Early impairment of hepatitis C virus specific T cell proliferation during acute infection leads to failure of viral clearance*. **Gut**, 2006; 55(7):1012-9.

13. Lechner F, Gruener NH, et al: *CD8+ T lymphocyte responses are induced during acute hepatitis C virus infection but are not sustained*. **Eur J Immunol,** 2000; 30(9):2479-87.

14. Grabowska AM, Lechner F, et al: *Direct ex vivo comparison of the breadth and specificity of the T cells in the liver and peripheral blood of patients with chronic HCV infection*. **Eur J Immunol**, 2001; 31(8):2388-9.

15. Wedemeyer H, He XS, et al: *Impaired effector function of hepatitis C virus-specific CD8+ T cells in chronic hepatitis C virus infection*. **J Immunol**, 2002; 169(6):3447-58.

16. Bengsch B, Seigel B, et al: *Coexpression of PD-1, 2B4, CD160 and KLRG1 on exhausted HCV-specific CD8+ T cells is linked to antigen recognition and T cell differentiation*. **PLoS Pathog**, 2010; 6(6):e1000947.

17. Blackburn SD, Shin H, et al: *Coregulation of CD8+ T cell exhaustion by multiple inhibitory receptors during chronic viral infection*. **Nat Immunol**, 2009; 10(1):29-37.

18. Nakamoto N, Cho H, et al: *Synergistic reversal of intrahepatic HCV-specific CD8 T cell exhaustion by combined PD-1/CTLA-4 blockade*. **PLoS Pathog**, 2009; 5(2):e1000313.

19. Radziewicz H, Ibegbu CC, et al: *Liver-infiltrating lymphocytes in chronic human hepatitis C virus infection display an exhausted phenotype with high levels of PD-1 and low levels of CD127 expression*. **J Virol**, 2007; 81(6):2545-53.

20. Sakaguchi S, Sakaguchi N, et al: *Immunologic tolerance maintained by CD25+ CD4+ regulatory T cells: their common role in controlling autoimmunity, tumor immunity, and transplantation tolerance*. **Immunol Rev**, 2001; 182:18–32.

21. Schwartz RH: *Natural regulatory T cells and self-tolerance*. **Nat Immunol**, 2005; 6:327-30.

22. Brunkow ME, Jeffery EW, et al: *Disruption of a new forkhead/winged-helixprotein, scurfin, results in the fatal lymphoproliferative disorder of the scurfy mouse*. **Nat Genet**, 2001; 27:68–73.

23. Hori S, Nomura T, and Sakaguchi S: *Control of regulatory T cell development by the Transcription factor Foxp3*. **Science**, 2003; 299:1057–61.

24. Karim M, Kingsley CI, et al: *Alloantigen-induced CD25+CD4+ regulatory T cells can develop in vivo from CD25-CD4+ precursors in a thymus independent process*. **J Immunol**, 2004; 172:923–8.

25. Lehtimäki S, and Lahesmaa R: *Regulatory T Cells Control Immune Responses through Their Non-Redundant Tissue Specific Features*. *Front Immunol*, 2013; 4:294.

26. Abbas AK, Benoist C, et al: *Regulatory T cells: recommendations to simplify the nomenclature*. **Nat Immunol**, 2013; 14(4):307-8.

27. Singer BD, King LS, and D'Alessio FR: *Regulatory T Cells as Immunotherapy*. **Front Immunol**, 2014; 11;5:46.

28. MacDonald AJ, Duffy M, Brady MT, et al: *CD4 T helper type 1 and regulatory T cells induced against the same epitopes on the core protein in hepatitis C virus-infected persons*. **J Infect Dis**, 2002; 185(6):720-7.

29. Boettler T, Spangenberg HC, et al: *T cells with a CD4+CD25+ regulatory phenotype suppress in vitro proliferation of virus-specific CD8+ T cells during chronic hepatitis C virus infection*. **J Virol**, 2005; 79:7860–67.

30. Rushbrook SM, Ward SM, et al: *Regulatory T cells suppress in vitro proliferation of virus-specific CD8+ T cells during persistent hepatitis C virus infection*. **J Virol**, 2005; 79: 7852–59.

31. Sugimoto K, Ikeda F, et al: *Suppression of HCV-specific T cells without differential hierarchy demonstrated ex vivo in persistent HCV infection*. **Hepatology**, 2003; 38(6): 1437-48.

32. Accapezzato D, Francavilla V, et al: *Hepatic expansion of a virus-specific regulatory CD8(+) T cell population in chronic hepatitis C virus infection*. J **Clin Invest**, 2004; 113(7):963-72.

33. Lenardo M, Chan KM, et al: *Mature T lymphocyte apoptosis—immune regulation in a dynamic and unpredictable antigenic environment*. **Annu Rev Immunol**, 1999; 17: 221–53.

34. Rouse BT, Suvas S: *Regulatory cells and infectious agents: détentes cordiale and contraire*. **J Immunol**, 2004; 173: 2211–15.

35. Belkaid Y, Piccirillo CA, et al: *CD4+CD25+ regulatory T cells control Leishmania major persistence and immunity*. **Nature**, 2002; 420: 502–07.

36. Langhans B, Krämer B, et al: *Intrahepatic IL-8 producing Foxp3⁺CD4⁺ regulatory T cells and fibrogenesis in chronic hepatitis C*. **J Hepatol**, 2013; 59(2):229-35.

37. Mahmood S, Sho M, et al: *Clinical significance of intrahepatic interleukin-8 in chronic hepatitis C patients*. **Hepatol Res**, 2002; 24(4):413-419.

38. Asselah T, Bièche I, et al: *Liver gene expression signature of mild fibrosis in patients with chronic hepatitis C*. **Gastroenterology**, 2005; 129(6):2064-75.

39. Claassen MA, de Knegt RJ, et al: *Abundant numbers of regulatory T cells localize to the liver of chronic hepatitis C infected patients and limit the extent of fibrosis*. **J Hepatol**, 2010; 52(3):315-21.

40. Sturm N, Thélu MA, et al: *Characterization and role of intra-hepatic regulatory T cells in chronic hepatitis C pathogenesis*. **J Hepatol**, 2010; 53(1):25-35.

41. Ward SM, Fox BC, et al: *Quantification and localisation of FOXP3+ T lymphocytes and relation to hepatic inflammation during chronic HCV infection.* **J Hepatol**, 2007; 47(3):316-24.

42. Marcos R, Monteiro RA, and Rocha E: *Design-based stereological estimation of hepatocyte number, by combining the smooth optical fractionator and immunocytochemistry with anti-carcinoembryonic antigen polyclonal antibodies*. **Liver Int**, 2006; 26(1):116-24.

43. F. D'Amico, A. Amoroso, et al: *Immunolocalization of FOXP3 in HCV-infected liver biopsies. Preliminary observations*. **EMC 2008** - 14th European Microscopy Congress, Aachen, Germany, 2008; pp 233-234.

44. Bode JG, Brenndörfer ED, and Häussinger D: *Hepatitis C virus (HCV) employs multiple strategies to subvert the host innate antiviral response*. **Biol Chem**, 2008; 389:1283-1298.

45. Flint M, and Tscherne DM: *Cellular receptors and HCV entry*. **Methods Mol Biol**, 2009; 510:265-277.

46. Manigold T, and Racanelli V: *T-cell regulation by CD4 regulatory T cells during hepatitis B and C virus infections: facts and controversies*. **Lancet Infect Dis**, 2007; 7:804-813.

47. Erhardt A, Biburger M, et al: *IL-10, regulatory T cells, and Kupffer cells mediate tolerance in concanavalin A-induced liver injury in mice*. **Hepatology**, 2007; 45:475-485.

48. Hall CH, Kassel R, et al: *HCV+ hepatocytes induce human regulatory CD4+ T cells through the production of TGF-beta*. **PLoS One**, 2010; 5:E12154.

49. Morgan ME, van Bilsen JH, et al: *Expression of FOXP3 mRNA is not confined to CD4+CD25+ T regulatory cells in humans*. **Hum Immunol**, 2005; 66:13-20.

50. Wang J, Ioan-Facsinay A, et al: *Transient expression of FOXP3 in human activated nonregulatory CD4+ T cells*. **Eur J Immunol**, 2007; 37:129-138.

51. Ward SM, Fox BC, et al: *Quantification and localization of FOXP3+ T lymphocytes and relation to hepatic inflammation during chronic HCV infection*. **J Hepatol**, 2007; 47: 316-324.

52. Wilczynski JR, Radwan M, and Kalinka J: *The characterization and role of regulatory T cells in immune reactions*. **Front Biosci**, 2008; 13: 2266-2274.

53. Vieira PL, Christensen JR, et al: *IL-10-secreting regulatory T cells do not express Foxp3 but have comparable regulatory function to naturally occurring CD4+CD25+ regulatory T cells*. **J Immunol**, 2004; 172: 5986-5993.

2. Phenotypical and functional markers in monitoring *ex vivo* expansion of clinical grade Cytokine-Induced Killers cells (CIK)

2.1 Introduction

Cell-based therapies represent nowadays an important and promising approach to onco-hematologic diseases and in regenerative medicine. Important results have already been obtained, and many others are at range. For these reasons this branch of science is currently object of intense research.

In onco-hematology, adoptive cell transfer of *ex vivo* expanded immune cells represents a therapeutic option, thanks to its properties to provide protection against post-transplant dangerous viral infections, as well as disease relapses, and to favour transplant engrafment (54). Post transplant-lymphocyte infusion, also named as donor lymphocyte infusion (DLI), finds in the *ex-vivo* expansion of Cytokine-Induced Killer cells (CIK) its most advanced and fascinating strategy to reach significant improvement in terms of disease-free survival, while reducing the frequency and severity of graft versus host disease (GVHD) (55).

As for other *Advanced Therapy Medicinal Products* (*ATMP*, as defined by the Regulation N° 1394/2007 of the European Parlament), the preparation of CIK cells has to face several bottlenecks for their development due to the complexity of the regulatory framework, the high costs and the needs for good manufacturing practice (GMP) facilities and new end-points for clinical experimentation. The study of optimal markers and systems for assessing the functionality of each batch of cellular product released is therefore of crucial importance.

One of the most challenging issues to be solved in the preparation of CIK cells is, in fact, a considerable inter-sample variability, which then leads to the expansion of products with variable features and properties, in terms of total cell number, cell phenotype and functional characteristics. Such differences can, in some cases, affect the final quality of the product. Thus, several efforts are presently being made in order to understand the reasons of this variability, as well as possible solutions or systems able to predict in advance the final outcome of the product.

2.2 Scientific background

Cytokine-Induced Killer cells (CIK). Cytokine-Induced Killer cells (CIK) are a heterogeneous bulk of ex-vivo expanded T lymphocytes. Thanks to their peculiar biological features they are considered the most promising choice for adoptive immunotherapy. Within the CIK culture it is possible to individuate three distinct cells populations: a $CD3^{+}CD56^{neg}$ cell subset, corresponding to T lymphocytes; $CD3^{neg}CD56^{+}$ Natural Killer cells, and a hybrid, newly generated subset, $CD3^{+}CD56^{+}$, which share the properties of both the other subsets.

CIK cells can classically be expanded starting from peripheral blood mononuclear cells (PBMC) but may also be generated from bone marrow or umbilical cord blood precursors (56). The standard culture condition, according to Negrin's protocol (57), requires three weeks with the timed addition of IFN-γ, anti-CD3 (OKT3) antibody and IL-2. IFN-γ is only added on day 0; its main activity is to activate the monocytes present in the initial bulk culture, which provide both contact-dependent (CD58/LFA-3) and soluble (IL-12) crucial signals that favour the acquisition of a final Th1 phenotype and the cytotoxic power of CIK cells. The anti-CD3 antibody provides mitogenic signals to T lymphocytes, subsequently sustained by IL-2 that drives the expansion.

Conventional $CD3^+CD56^{neg}$ T cells present in the final CIK bulk are mostly $CD8^+$, though also other, less represented, subsets like $CD4^+$ T Helper, double-negative $CD4^{neg}CD8^{neg}$ and double-positive $CD4^+CD8^+$ can be found; all these subsets display a low cytotoxic ability but a high proliferative potential (54).

Unlike $CD3^+$ T cells, $CD3^{neg}CD56^+$ NK cell subset shows the typical features of activated *Lymphokine-Activated Natural Killer* cells (LAK): they display high cytotoxicity *in vitro* against different cell lines, but a short survival when infused in-vivo; in fact, the most important limit for the clinical use of pure NK cells is their great dependence on high levels of IL-2 that cannot be administered *in vivo* for long term (58).

Finally, the $CD3^+CD56^+$ cell subset shows a higher cytotoxicity and longer survival capacity compared to Natural Killer cells; $CD3^+CD56^+$ NKT cells are able to lyse different lines of cancer cells in a NK-like manner, and are estimated the major responsible for MHC-unrestricted antitumor activity (59). They display basically a terminally differentiated, late-effector phenotype ($CD45RO^+$ $CD27^{low}$ $CD28^{low}$ $CD62L^{neg}$ $CCR7^{neg}$). Interestingly, they keep TCR-mediated activation and function, and are shown to display an antigen-specific recognition and killing of target cells. This property is of particular importance, as it has two implications. First, the retaining of a totally functioning TCR makes NKT cells less dependent on IL-2 stimuli compared to the high levels needed to maintain the activation of NK cells; NKT cells can, in fact, be stimulated by antigens or by CD3-targeted antibodies. Second, the antigen specificity could further be exploited by expanding antigen-selected clones of precursors, for example, specific for CMV or other opportunistic pathogens that are cause of dangerous, post-transplant infections and mortality (54). It is actually well known that, within the CIK bulk, NKT cells precursors are $CD3^+$ T lymphocytes mainly with a naïve, $CD4^{neg}CD8^{neg}$ double negative phenotype that eventually, upon stimulation, acquire the $CD3^+CD56^+$ phenotype (60).

CIK's open challenges: clinical translation. An important limitation preventing the successful clinical translation of several adoptive immunotherapy strategies is the difficulty in obtaining sufficient numbers of anti-tumor immune effectors and their short *in vivo* persistence after infusion into the patients. Compared to other adoptive

immunotherapy strategies, the main functional properties that favourably characterize CIK cells are their easy *ex vivo* expansion, their MHC-unrestricted tumor killing ability and their low alloreactivity (58). Their reduced alloreactive potential across MHC barriers may result in a reduced risk for GVHD if adoptively infused after allogenic Hemopoietic Stem Cell Transplant (HSCT).

The data present in literature, are in favour of a possible use of CIK as an alternative to traditional Donor Lymphocyte Infusion (DLI) following allogenic HSCT. However, despite *in vitro* studies showed a lower alloreactivity potential for CIK cells, initial clinical trials infusing donor CIK cells after HLA identical HSCT, reported a 36% of GVHD incidence (61). However, further studies have shown how such alloreactivity is basically attributable to the $CD3^{+}CD56^{neg}$ fraction of CIK's bulk (59). A depletion of this population could therefore lead to a reduction of GVHD incidence and strength. This approach might be of particular relevance in peculiar HSCT settings with a partial HLA-mismatch. It is, however, worth to mention that the $CD3^{+}CD56^{neg}$ subset in the CIK bulk is the one that retains the highest proliferative potential, and that might therefore represent a source of $CD3^{+}CD56^{+}$ generation in vivo, after infusion.

CIK cells show particular flexibility in their mechanisms of action, as many redirection cytotoxicity experiments show; other intriguing perspectives for CIK-based adoptive immunotherapies are given by the emerging possibilities to redirect and potentiate their antitumor activity with the auxilium of Tumor-Associated Antigens (TAA) – bispecific antibodies (62). Recently, CIK-based adoptive immunotherapy has been proposed for solid tumors, and clinical trials have started (58).

In general, the heterogeneity of methods and response evaluation criteria make the drawing of definitive conclusions regarding impact on survival still early and difficult. Recently, an International Registry on CIK Cells (IRCC) has been created, with the aim to collect worldwide data on clinical trial results (63).

CIK's open challenges: batch variability. The standards for optimal CIK expansion have been currently successfully validated under Good Manufacture Practice (GMP) conditions (56). However, after three weeks of culture the expansion rate is reported to be variable, from few

to more than 1000 fold (64). The reasons of this great variability in the expansion rate are still not known, but their understanding would be of great importance, as the highest levels of expansions are largely feasible for further clinical applications: some batches behave as "poor expanders", and might benefit from additional biological stimuli. Soluble factors like Thymoglobulin, IL-1 or IL-7 have been considered to be used, as well as the addition of transient allogenic stimulation (delivered by irradiated allogenic PBMC) or the depletion of regulatory T cells. Recent studies, in the attempt to shed light on the causes of such a high variability, have employed multivariate statistical data analysis algorithms, in order to predict the final outcome of a single batch (64).

Moreover, as CIK cells are often expanded starting from PBMC, interesting studies have focused the attention on the other populations present in the initial PBMC culture, like monocytes and residual granulocytes, which could theoretically influence the outcome of CIK expansion. Activated neutrophils have been shown to be able to increase cytotoxic activity of both NK and T cells (65-69). The role of monocytes is, on the other hand, still controversial (70, 71): experiments using the transwell system showed that the stimulatory effect of autologous PBMC on activated NK cells resides in the $CD14^+$ monocyte fraction; proliferation is in part mediated by humoral factors, but is enhanced when NK and monocytes are in direct cell-cell contact (70). In other experimental settings, monocytes inhibited the proliferation of NK and T cells during IL-2 co-culture for 7, 14, or 21 days. A reduction in monocytes resulted in a 61-fold expansion of NK cells and a 3,7-fold increase of T cells (71).

Other studies point out how differences in the isolation procedures might be responsible for significant functional differences in the final cellular product, and delays in processing beyond 8 hours can result in early activation of cells, decreased chemokine receptor expression, or decreased ability of NK cells to degranulate or secrete cytokines. Notably, Seeger and co-workers compared the methods for the preparation of bone marrow-derived mononuclear cells (BM-MNC) in the REPAIR-AMI and ASTAMI trials (72). In the experiments described, the authors found significant differences between the cell recoveries obtained using the two products, a difference which was the

only discernible reason for the differences observed for the number of $CD45^+/CD34^+$ BM-MNC, CFU, and MSC (72).
In line with these findings, the assessment of cell number and viability may not entirely reflect the functional capacity of cells in vivo, and additional functional testing appears to be mandatory to assure proper cell function before embarking on clinical cell therapy trials (73).

2.3 Study design

Given these open issues, the aim of this preliminary study was to acquire further information on the phenotypical and functional features of *ex vivo* expanded Cytokine-Induce Killer cells (CIK), when cultured under different experimental variables. In particular, the expansion of cells obtained from different density gradient separation reagents was tested, by applying different phenotypical and functional tests such as total cell count, cell viability, cell separation purity and recovery, cell surface flow cytometry staining, calcein-release cytotoxicity assay and flow cytometry-based cell cycle analysis.

2.4 Materials and methods

Sample collection. PBMCs were isolated from 4 buffy coats obtained from regular healthy donor whole blood donations. After donation, buffy coats were obtained by centrifuging the blood bags in order to obtain blood separation into three components: plasma, concentrated erythrocytes and buffy coat (containing most leucocytes and platelets). The separation procedure was performed to obtain transfusional products for clinical use, according to Italian transfusion medicine operative standards. The concentrated erythrocytes and plasma components contemporarily obtained by the separation were regularly employed for clinical purpose. Informed consent about the different destination (*in vitro* use) of the buffy coats was asked for and obtained by each donor. No additive amount of blood collection was required, compared to a normal blood donation.

Isolation of PBMC. PBMC were obtained by density gradient centrifugation of the buffy coats. For the study purpose, 4 different density gradient centrifugation reagents were used for each buffy coat (*Ficoll-Paque PLUS*, GE Healthcare, UK; *Histopaque – 1077*, Sigma-Aldrich, USA; *Biocoll*, Biochrom – Merck Millipore, Germany; *Lymphoprep*, Axis-Shield, Norway).

Pre-isolation leukocyte concentration was assessed by a diagnostic emocytometer (ADVIA 120 Hematology System, Siemens, Germany) from each buffy coat, in order to calculate the recovery rate of each separation reagent. The average leukocyte concentration was over 25.000 / mm^3 (range 28-38 x 10^8). On the basis of preliminary experiments, it was established that 4 ml of buffy coat for each isolation condition would have been sufficient to obtain the required amount of cells for all experiments. Samples were also analyzed for their immunophenotype in flow cytometry prior to separation (see paragraph 2.4 – *Immunophenotypical analysis in flow cytometry*).

A careful comparison of the manufacturer's instructions of the four reagents was conducted prior to set the experiment plan. However, only minor differences were found among the recommended operative procedures, while all the four manufacturers did not point out strict indications about the optimal buffy coat dilution to obtain the best separation. For these reasons, we established that a unique operative procedure and a dilution of 1:4 were feasible for all the four separation reagents.

For each sample, PBMC were isolated by using all the four separation reagents used (as explained above). For each experimental condition, two 15 ml polypropylene tubes were firstly filled with 6 ml of density gradient separation reagent; subsequently, 8 ml of [1:4-DPBS]-diluted buffy coat were added slowly, not to disrupt the separation between the two liquid phases.

Samples were centrifuged at 800 rcf (without brake) for 30 minutes. After centrifugation, separated PBMC were recovered from the tubes, counted by using *Trypan blue exclusion test* in a Bürker haematological chamber in optical microscopy, washed, analyzed in flow cytometry for their phenotype, and resuspended in *X-VIVO-10* medium (Lonza, Switzerland).

Determination of cell recovery, purity and viability. Cell recovery was obtained by calculating the percentage from the cell number obtained after density gradient separation referred to the number of cells which underwent separation. The expected recovery of lympho-monocyte population was also calculated, by using the data obtained from a diagnostic emocytometers on buffy coat samples (ADVIA 120 Hematology System, Siemens, Germany). The purity of the isolated population of lymph-monocytes was estimated by flow cytometry analysis (see below, *Immunophenotypical analysis in flow cytometry*). Viability of cells was assessed by *Trypan blue exclusion test* in a Bürker haematological chamber in optical microscopy.

CIK cell culture and expansion. PBMC isolated from each separation reagent were counted and resuspended in X-VIVO-10 medium at a concentration of $5x10^6$ cells/ml. 25 x 10^6 cells (in 5 ml volume) for each condition were then seeded in a different 12,5 cm^2 culture flask. The stimulation schedule, according to Negrin's protocol, consisted in the addition of 1.000 U/ml of IFN-γ (*Imukin* - Boehringer-Ingelheim, Germany) at day 0, 50 ng/mL of Anti-CD3 (Pure functional grade - Miltenyi Biotec, Germany) at day 1, and 500 U/ml of IL-2 (*Proleukin*, Novartis Pharma, Switzerland) at days 1, 3, 7, 10, 14 and 17. Cells were incubated for 21 days at 37°C, 5% CO_2, in humidified atmosphere. Cell concentration was determined at days 3, 7, 10, 14, 17, 21. After every cell count estimation, incubation was continued at a cell concentration of $1x10^6$ cells/ml. No washing step was performed; fresh medium was added to lower the concentration. Starting from day 3, cells were seeded in 25 cm^2 culture flasks ($1x10^7$ cells in 10 ml volume).

Immunophenotypical analysis in flow cytometry. Immunophenotypical analysis was performed by using a Beckman Coulter Cytomix FC500 flow cytometer. Cells were analyzed at day 0 (before and after gradient separation), and at days 3, 7, 10, 14, 17 and 21. The fluorescent monoclonal antibodies used were directed against CD3 (ECD-conjugated), CD4(-FICT), CD8(-PECy7), CD56(-PE), CD14(-PE),

CD33(-APC), CD19(-PECy7) surface antigens. All antibodies were provided by Beckman Coulter (USA).

Calcein release cytotoxicity assay. Cytotoxicity of CIK cells was assessed at days 7, 14 and 21, by calcein-release fluorimetric assay. K562, a human chronic myeloid leukemia cell line was chosen as target (K562, subclone ACC10, purchased by DSMZ, GmbH, Germany). Briefly, 10^6 K562 cells were resuspended in 5 ml of 10% FBS RPMI medium and incubated with 3,5 μM calcein AM (acetoxymetyl-estere, Sigma-Aldrich, Switzerland); after a washing step, labelled cells were resuspended in X-VIVO-10 at a concentration of $5x10^4$ cells/ml. Effector cells were washed and resuspended at three different concentrations ($2x10^6$, $1x10^6$ and $5x10^5$ cells/ml) in X-VIVO-10. Effector-to-target ratios tested were 10:1, 20:1, 40:1. For the co-incubation with target cells, a 96-well plate was used: 100 μl of the three different concentrations of effectors cells were placed in the wells, and 100 μl of target cell suspension were added to reach the required E:T ratio. Incubation was performed for 4 hours at 37°C, 5% CO_2, in humidified atmosphere. All samples were run in duplicate. Four wells with target cells alone (100 μl) were used as negative control, to assess the basal release; to assess the maximal calcein release, four more wells with 100 μl of target cells alone were prepared and 100 μl of 3% TRITON 100X were added at the end of incubation.
After incubation cells were centrifuged and placed in a black/transparent bottom 96 well plate. The RFU (*Relative Fluorescence Units*) were obtained by reading the plate with a *BF1000 FluoroCount* fluorimeter (λ-excitation 485 nm / λ-emission 535 nm, Packard Bioscience, USA).

Cell cycle analysis in flow cytometry. Cell cycle analysis was performed in flow cytometry by using the protocol established by Carbonari and coworkers in 2008 (19), named FAST (*Flow Acetone-Staining Tecnique*). 7-amino-actinomycin (7-AAD) was used as intercalating agent (λ-excitation 543 nm / λ-emission 647; 10 μg/ml final concentration).
Collected data were analyzed by the *Multiple AV* software (Phoenix Flow Systems, San Diego, CA).

Fold expansion estimation. Fold expansion estimation was obtained by multiplying the number of cells counted at every checkpoint (day 0, 3, 7, 10, 14, 17, 21) for the number of cells obtained at the preceding checkpoint. Noteworthy, as the starting concentration (day 0) was 5 x 10^6 cells/ml, the number of cells at day 3 was divided by 5, to normalize the starting count at 1 x 10^6 cells/ml.

Statistical analysis. Statistical analysis of collected data was performed by using the *Prism 5* software (Graphpad, USA). The difference among the data from the four different separation reagents were tested for significance. ANOVA test was used, along with Tukey's post-test for multiple one-to-one comparisons among the separation reagents. p value <0,05 was considered as statistically significant. Data are expressed as mean ± sd.

2.5 Results

Cell recovery, purity and viability. The overall recovery estimation from the four experimental conditions showed that *Ficoll-Paque PLUS* (GE Healthcare) exhibited a significantly lower recovery rate (54,3± 3,3%); the other reagents did not show statistically significant differences (Fif. 6/A). The expected recovery of lympho-monocyte population ranged from a minimum of 96,3% (Sample 3 / GE-Healthcare) to a maximum of 99,9% (Sample 1 / Axis-Shield), without significant differences (data not shown). Purity of the isolated lympho-monocyte populations was inversely correlated to the presence of residual granulocytes and proved to be significantly lower in the cell suspension obtained from Axis-Shield reagent (Fig. 6/B). Although without statistically significance, the highest purity was observed on the GE-Healthcare-derived cell suspension. Cell viability was comprised from a minimum of 93,5% (Sample 2 / Biochrom) to a maximum of 98,6% (Sample 3 / Axis-Shield) without significant differences (data not shown).

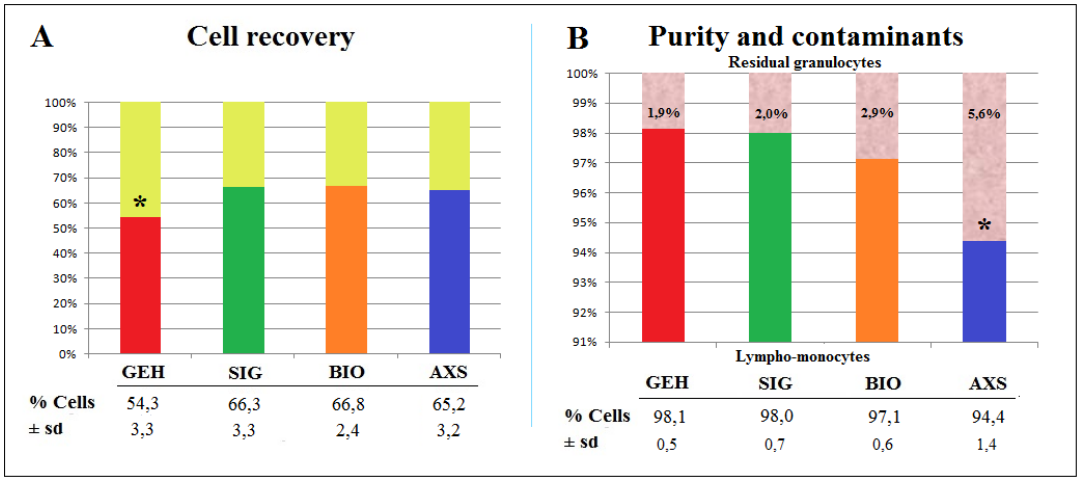

Fig 6. Recovery and purity rate of the four different separation reagents
(Data are expressed as mean ± standard deviation)**.**

Phenotypical features of the isolated population. Regarding the initial presence of monocytes and B lymphocytes, no statistically significant differences were observed among the four reagents. Table 3 shows the mean percentages of B cells and monocytes in the cell suspensions obtained after the density gradient separation performed by using the 4 different reagents. By the course of the culture their percentage dramatically fell down, as well as the one of granulocytes. At the third day of culture the percentage of granulocytes and monocytes became undetectable in all cultures (data not shown), while B cell percentage were detectable until day 14 (Fig. 7).

Percentages of unwanted cells after density gradient separation (day 0; values are indicated as mean ± s.d.)			
	B lymphocytes	**Monocytes**	**Granulocytes**
GEH	6,6 ± 2,9%	8,3 ± 2,8%	1,9 ± 0,5%
SIG	7,0 ± 2,7%	9,3 ± 3,6%	2,0 ± 0,7%
BIO	5,9 ± 2,0%	8,8 ± 1,9%	2,9 ± 0,6%
AXS	7,7 ± 3,0%	9,4 ± 2,9%	5,6 ± 1,4%

Table 3. Percentages of contaminant populations after density gradient separation.

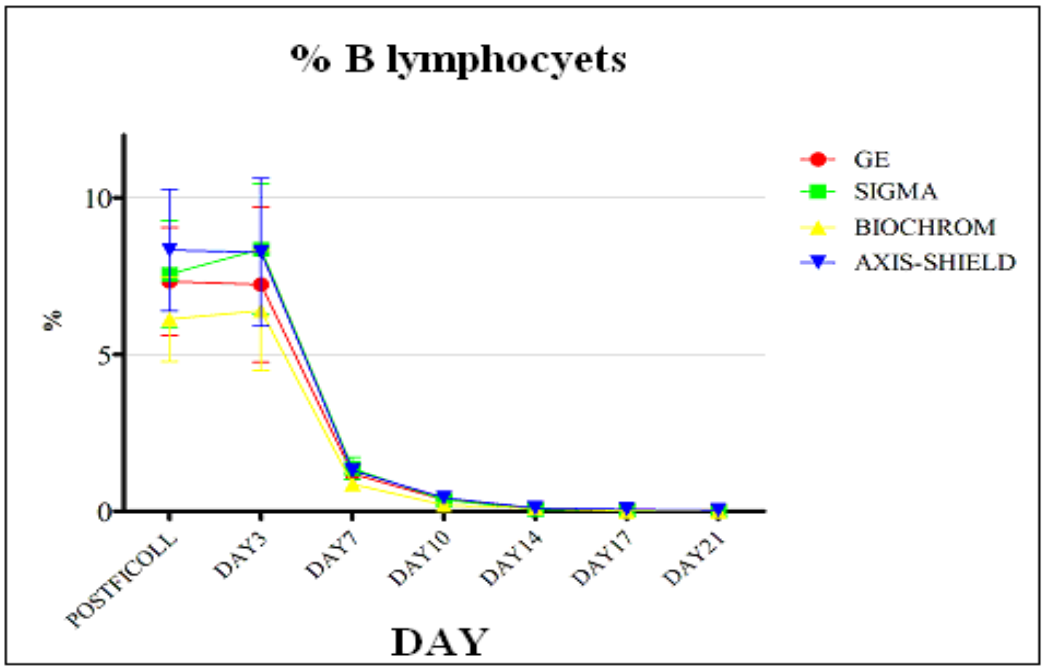

Figure 7. Percentage of B cells in the expanding culture.

As expected, the starting T cell population was constituted by a majority of $CD3^{+}CD56^{neg}$ cells, whereas cells with Natural Killer phenotype ($CD3^{neg}CD56^{+}$) and naive 'double-positive' $CD3^{+}CD56^{+}$ cells represented minor populations. No statically significant differences were detected among the cell suspensions obtained from the four reagents. The percentages of the different cell populations along the culture days are shown in Figure 8 and 9.

CIK expansion. Figure 8 shows the growing curve of $CD3^{+}CD8^{+}$ and $CD3^{+}$ $CD4^{+}$ cells during the culture days under the four different experimental conditions; figure 9 shows the growing curve of $CD3^{-}$ $CD56^{+}$ and $CD3^{+}CD56^{+}$ cells; table 4 shows the mean percentages of the these populations (± s.d.) at the end of the culture, under the four different experimental conditions.

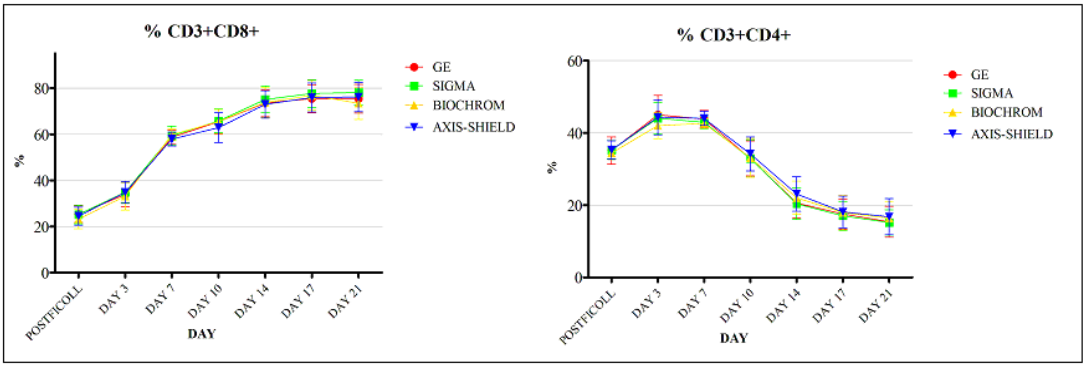

Figure 8. $CD8^+$ and $CD4^+$ T cell subset growing curve along CIK expansion.

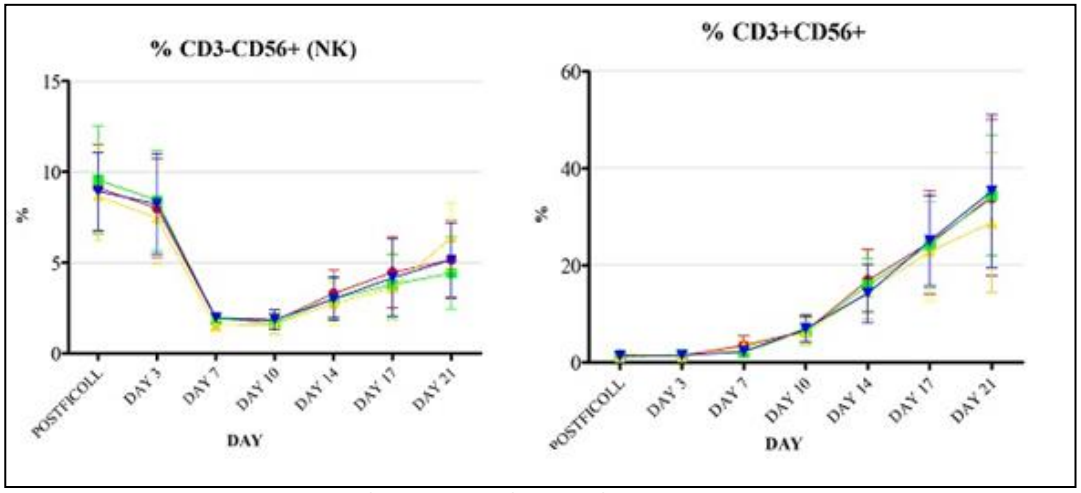

Figure 9. $CD3^{neg}CD56^+$ and $CD3^+CD56^+$ cell growing curve along CIK expansion.

Percentages of cell subsets constituting CIK bulk at the end of the culture (day 21; values are indicated as mean ± s.d.)			
	CD3+CD8+	CD3-CD56+	CD3+CD56+
GEH	75,3 ± 8,4%	5,2 ± 2,1%	34,0 ± 16,1%
SIG	74,9 ± 9,5%	4,4 ± 2,0%	34,5 ± 12,4%
BIO	72,2 ± 10,6%	6,4 ± 1,9%	28,9 ± 14,4%
AXS	73,6 ± 8,8%	5,2 ± 2,0%	35,3 ± 15,8%

Table 4. Percentages of cell subsets constituting CIK bulk at the end of the culture.

$CD3^+CD4^+$ T helper cells show an initial increase due to the stimulation mediated by IFN-γ, anti-CD3 and IL-2. However, on further days, their percentage shows a decrease due to their incapacity to proliferate in the presence of IL-2 only.
At day 21 of the culture, the major population is represented by $CD3^+CD8^+$ T cells, a variable but significant portion has shown to be also $CD56^+$ (data not shown). The culture derived from Biochrom separation reagent shows lower percentage of $CD3^+CD56^+$ cells: statistical analysis reveals that this difference is significant in 2 sample out of 4 ($p<0.05$). The growing curve of $CD3^+CD56^+$ cells obtained from Biochrom reagent showed also a deceleration starting from day 17 (figure 9).
The percentage of $CD3^{neg}CD56^+$ Natural Killer cells showed no statistical significance (figure 9).

Cytotoxicity assays. Cytotoxicity of CIK cells increased from day 7 to day 21, in all experimental conditions. The increase in cytotoxic activity was more dramatic between day 7 and day 14. Although the data obtained did not reach a statistical significance, the CIK population obtained from Biochrom reagent showed a lower mean cytotoxicity compared to the others (figure 10).

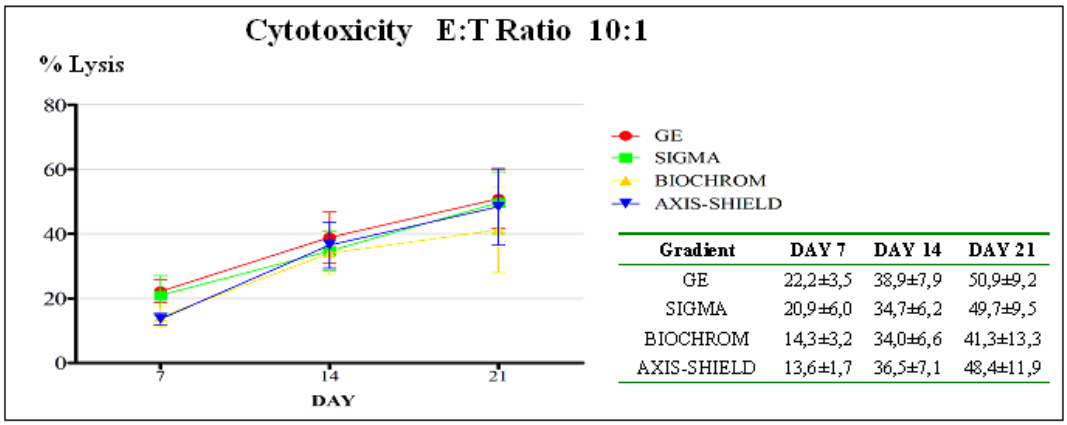

Gradient	DAY 7	DAY 14	DAY 21
GE	22,2±3,5	38,9±7,9	50,9±9,2
SIGMA	20,9±6,0	34,7±6,2	49,7±9,5
BIOCHROM	14,3±3,2	34,0±6,6	41,3±13,3
AXIS-SHIELD	13,6±1,7	36,5±7,1	48,4±11,9

Figure 10. Cytotoxicity assay across culture days (E:T 10:1).

Cell cycle, and fold expansion. Cell cycle analysis revealed a progressive decrease of cells undergoing active DNA synthesis along the culture (Figure 11), showing that the the highest proliferation occurred during the first two weeks of culture. No significant difference could be appreciated among the four experimental conditions.

Fold expansion ranged from a minimum of 14,9 (Sample 1/Biochrom) to a maximum of 221,7 (Sample 3/GE); the mean values did not show significant difference (Figure12).

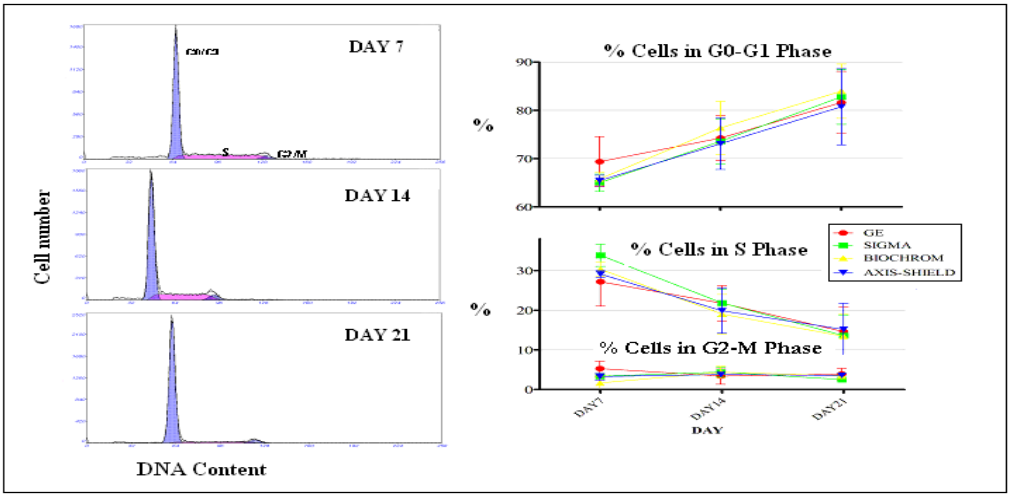

Figure 11. Analysis of cells cycle along culture days.

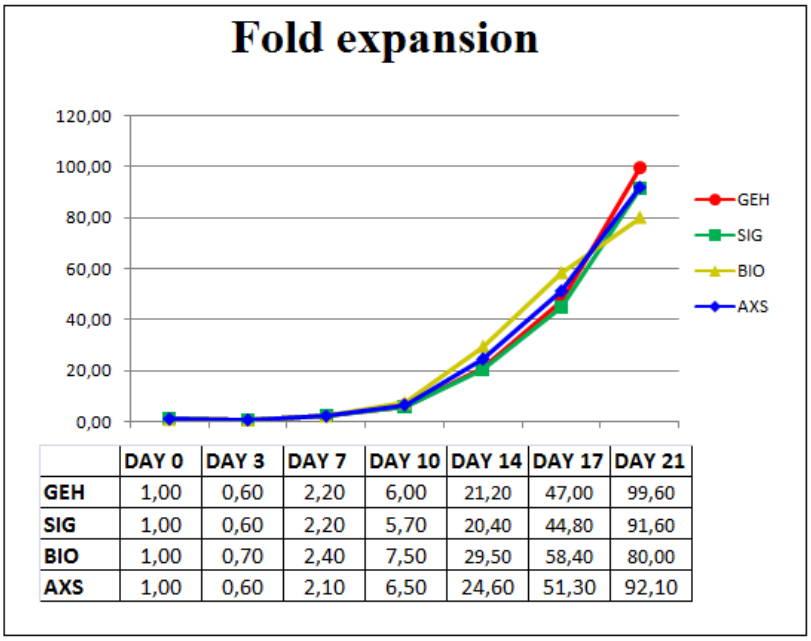

	DAY 0	DAY 3	DAY 7	DAY 10	DAY 14	DAY 17	DAY 21
GEH	1,00	0,60	2,20	6,00	21,20	47,00	99,60
SIG	1,00	0,60	2,20	5,70	20,40	44,80	91,60
BIO	1,00	0,70	2,40	7,50	29,50	58,40	80,00
AXS	1,00	0,60	2,10	6,50	24,60	51,30	92,10

Figure 12. Expansion curve and mean fold expansion values.

2.6 Discussion

The high variability of CIK expansion results, in terms of fold expansion and cell functionality, render CIK protocol translation into clinical settings difficult. Despite CIK expansion protocol has already been validated under Good Manufacture Practice (GMP) conditions (56), further optimizations in order to reduce such variability are still possible; thus, further validations studies should be programmed.

The application of functional tests in the present study, to monitor different features of CIK cells along their expansion, has revealed how minor variables, even the first isolation step, can lead to significant differences in terms of composition and functionality of expanded cells. The use of density gradient separators is a very common laboratory practice, though the choice of the reagent to be employed is often a minor issue, mainly dependent on economical matters. However, as also previous studies have stated, processing variations might be able to completely change the conclusion of a study (73); great attention should therefore be paid especially when the complete functional capacity of cells is essentially required.

In our preliminary study, despite the number of the samples collected was low, a statistically significant correlation could be established for some critical aspects, such as post-separation cell recovery, purity, and population doubling. For other data sets, such as percentage of $CD3^{+}CD56^{+}$ cells along the culture days, CIK cell fold expansion and cytotoxicity, although a statistical significance was not reached, a clear and univocal information emerged, suggesting the idea that a higher sample number could provide the statistical confirmation. In particular, GE-Healthcare reagent granted the strictest selectivity (lowest recovery rate and lowest residual contaminants), but its performance was among the highest as for population doubling and citotoxicity. On the other hand, Biochrom reagent performance often tended to be at the lowest levels, in terms of fold expansion and citotoxicity; moreover, cells isolated by this reagent saw a decrease in their expansion starting from day 17. As the number of precursors was the same for all experimental conditions and no exuberant numbers of contaminant cells could be detected after using Biochrom reagent compared to others, it is possible to postulate that this reagent has a negative impact on the functionality

of stimulatory membrane receptors. This is particularly important when the in vivo functionality is considered; it is worth to remember that in vitro cytotoxicity against K562 cell line depends greatly on the activity of $CD3^{neg}CD56^{+}$ Natural Killer fraction of CIK cells; *in vivo*, on the contrary, the cytotoxic activity seems to be dependent mostly on the number and functionality of $CD3^{+}CD56^{+}$ population: the *in vivo* impact of a separation reagent which grants suboptimal expansion and longevity of the $CD3^{+}CD56^{+}$ fraction could therefore negatively influence the functional response of the final cellular product. A technical consequence of this outcome is finally that alternative systems for assessing citotoxicity, more sensible and non uniparametric, such as flow cytometry based assays, should be taken as an important option, as they could more faithfully estimate and foresee the real *in vivo* functionality of cells.

2.7 Conclusions

In conclusion, the *ex vivo* expansion of Cytokine-Induced Killer cells (CIK) for clinical applications is affected by a high inter-sample variability of cell functionality which delays the entry of this product into clinical settings. Further validation studies are therefore necessary in order to understand the causes of such a high variability. Of note, different processing variations such as the use of a specific density gradient separation reagent, could play a role in the suboptimal level of cell expansion and citotoxicity, as they could be able to influence the crosstalk among the different cellular subsets present in the CIK bulk. The use of appropriate phenotypical and functional tests used in combination to assess cell behaviour during the entire expansion process could be able to provide the scientist the right clues to orient the optimization process.

2.8 References

54. Sangiolo D, Mesiano G, et al: *Cytokine induced killer cells as adoptive immunotherapy strategy to augment graft versus tumor after hematopoietic cell transplantation*. **Expert Opin Biol Ther**, 2009; 9(7):831-40.

55. Slavin S, Morecki S, et al: *Donor lymphocyte infusion: the use of alloreactive and tumor-reactive lymphocytes for immunotherapy of malignant and nonmalignant diseases in conjunction with allogeneic stem cell transplantation*. **J Hematother Stem Cell Res**, 2002; 11(2):265-76.

56. Introna M, Franceschetti M, et al: *Rapid and massive expansion of cord blood-derived cytokine-induced killer cells: an innovative proposal for the treatment of leukemia relapse after cord blood transplantation*. **Bone Marrow Transplant**, 2006; 38(9): 621-7.

57. Alvarnas JC, Linn YC, at al: *Expansion of cytotoxic CD3+ CD56+ cells from peripheral blood progenitor cells of patients undergoing autologous hematopoietic cell transplantation*. **Biol Blood Marrow Transplant**, 2001; 7(4): 216-22.

58. Sangiolo D: *Cytokine Induced Killer Cells as Promising Immunotherapy for Solid Tumors*. **J Cancer**, 2011; 2:363-8.

59. Sangiolo D, Martinuzzi E, et al: *Alloreactivity and antitumor activity segregate within two distinct subsets of Cytokine-induced killer (CIK) cells: implications for their infusion across major HLA barriers*. **Int Immunol**, 2008; 20(7): 841-8.

60. Lu PH and Negrin RS: *A novel population of expanded human CD3+CD56+ cells derived from T cells with potent in vivo antitumor activity in mice with severe combined immunodeficiency*. **J immimunol**, 1994; 153(4): 1687-96.

61. Introna M, Borleri G, et al: *Repeated infusions of donor-derived cytokine-induced killer cells in patients relapsing after allogeneic stem*

cell transplantation: a phase I study. **Haematologica**, 2007; 92(7):952-9.

62. Verneris MR, Arshi A, et al: *Low levels of Her2/neu expressed by Ewing's family tumor cell lines can redirect cytokine-induced killer cells*. **Clin Cancer Res**, 2005; 11(12):4561-70.

63. Hontscha C, Borck Y, et al: Clinical trials on CIK cells: first report of the international registry on CIK cells (IRCC). J Cancer Res Clin Oncol, 2011; 137(2): 305-10.

64. Zanon C, Stocchero M, et al: *Multivariate statistical data analysis as a tool to analyze ex vivo expansion dynamics of cytokine-induced killer cells*. **Cytometry B Clin Cytom**, 2014; 86(4):257-62.

65. Mantovani A, Cassatella MA, et al: *Neutrophils in the activation and regulation of innate and adaptive immunity*. **Nat Rev Immunol**, 2011; 11(8): 519-31.

66. Jaeger BN, Donadieu J, et al: *Neutrophil depletion impairs natural killer cell maturation, function, and homeostasis*. **J Exp Med**, 2012; 209(3): 565-80.

67. Costantini C, Calzetti F, et al: *Human neutrophils interact with both 6-sulfo LacNAc+ DC and NK cells to amplify NK-derived IFN{gamma}: role of CD18, ICAM-1, and ICAM-3*. **Blood**, 2011; 117(5): 1677-86.

68. Costantini C, Micheletti A, et al: *On the potential involvement of CD11d in co-stimulating the production of interferon-γ by natural killer cells upon interaction with neutrophils via intercellular adhesion molecule-3*. **Haematologica**, 2011; 96(10):1543-7.

69. Tillack K, Breiden P, et al: *T lymphocyte priming by neutrophil extracellular traps links innate and adaptive immune responses*. **J Immunol**, 2012; 188(7): 3150-9.

70. Miller JS, Oelkers S, et al: *Role of monocytes in the expansion of human activated natural killer cells*. **Blood**, 1992; 80(9): 2221-9.

71. Ageitos AG, Singh RK, et al: *IL-2 expansion of T and NK cells from growth factor-mobilized peripheral blood stem cell products: monocyte inhibition*. **J Immunother**, 1998; 21(6): 409-17.

72. Seeger FH, Tonn T, et al: *Cell isolation procedures matter: a comparison of different isolation protocols of bone marrow mononuclear cells used for cell therapy in patients with acute myocardial infarction*. **Eur Heart J**, 2007; 28(6): 766-72.

73. Naranbhai V, Bartman P, et al: *Impact of blood processing variations on natural killer cell frequency, activation, chemokine receptor expression and function*. **J Immunol Methods**, 2011;366(1-2): 28-35.

74. Carbonari M, Mancaniello D, et al: *Flow acetone-staining technique: a highly efficient procedure for the simultaneous analysis of DNA content, cell morphology, and immunophenotype by flow cytometry*. **Cytometry A**, 2008; 73(2): 168-74.

3. Nectin-like-5 expression correlates to malignant phenotype in cutaneous melanoma

3.1 Introduction

Malignant melanoma arises from the transformation and proliferation of melanocytes that are normally found in the basal cell layers of epidermis. It is the most deadly form of skin cancer, deriving from de novo melanocyte transformation in 75% of the cases and from preexisting nevi in 25% of the cases. Melanoma accounts for less than 5% of skin cancers but is responsible for 80% of skin cancer related deaths.

The pathogenesis of melanoma is a complex phenomenon in which environmental, genetic, and host factors are involved. Several studies have shown how alterations in the expression of molecules involved in motility and cellular crosstalk are one of the most important pathological events leading to the development of melanoma tumors. From these events depend the ability and the propension of transformed cells to give metastasis. The list of the effectors includes cell-cell and cell adhesion molecules, matrix-degrading enzymes, cytokines and other cleavage-derived motility factors, growth factors and their receptors. Malignant melanoma is an excellent model for studying these molecules, due in part to a sequential series of defineable stages. As the malignant phenotype of melanoma cells changes from the noninvasive radial growth phase to the vertical growth phase, which has high metastatic potential, the repertoire of the cellular adhesion molecules changes.

Recently, a growing interest has been focused on new cellular crosstalk molecular systems, such as the lectin families. In particular, Nectin-like molecule 5 (Necl-5), also known as Polio Virus Receptor (PVR) or

CD155, has come to the first line of scientific interest thanks to its multiple functions. As a nectin molecule, its primary function seems to be the regulation of cell-cell cross talk. Several studies have demonstrated that Necl-5 overexpression in cancer cells is essential for migration, invasion, proliferation and metastasis formation abilities, but there is not yet enough evidence about the possible use of this molecule as a biomarker, nor as a target for possible therapeutic approaches.

3.2 Scientific background

Melanoma overview. Cutaneous metastatic melanoma (CMM) is the most deadly form of skin cancer, deriving from de novo melanocyte transformation in 75% of the cases and from preexisting nevi in 25% of the cases. Melanoma accounts for less than 5% of skin cancers but is responsible for 80% of skin cancer related deaths. Melanoma incidence in Caucasian population has increased dramatically worldwide during the past several decades (75). Melanoma is a cancer with a relatively good prognosis when diagnosed early at a cutaneous localized stage. Patients with thin lesions can usually be cured with surgical excision. Their 5-year survival rate ranges from 90% to 100%. However, the prognosis worsens the deeper the lesion extends below the skin, because of melanoma's propensity to invade and to form metastasis. Individuals with thick melanomas have an increased risk to develop lymph node and visceral metastases. Metastatic melanoma cannot be completely removed by surgery and metastatic cells display extreme resistance to all types of treatment. Patients with metastatic melanomas have a median survival rate that typically ranges from six to ten months (76).

The genesis of melanoma is a complex phenomenon in which environmental, genetic, and host factors are involved. Recent data reveal that melanomas are heterogeneous tumors, harboring various genetic alterations, developing at different body sites and on sun-exposed and non sun-exposed regions, suggesting that melanoma arises from divergent causal pathways. Curtin and coworkers proposed a

molecular classification based on the sites where melanoma occurs, the genetic alterations and the sun exposure history (77).
Malignant melanoma arises from the transformation and proliferation of melanocytes that are normally found in basal cell layer of the epidermis. Tumor growth can be biphasic or monophasic (78). The biphasic pattern consists of a horizontal or radial initial growth phase (RGP) followed by a subsequent vertical growth phase (VGP) corresponding to the infiltration of the dermis and hypodermis. The monophasic growth pattern of melanoma consists of pure vertical growth mode. When the lesion enters the vertical growth phase, the repertoire of adhesion molecules changes as the tumor enters the dermis and acquires the capacity to metastasize. Genetic alterations including inactivation of the INK4a/ARF melanoma susceptibility locus, activating mutations in RAS/B-RAF oncogenes, alterations/loss of PTEN, p53 mutations, and CDK4 mutations occur early during melanoma development (79, 80).

Cellular crosstalk in melanoma. In normal skin, melanocytes are found as single cells scattered among keratinocytes at the epidermal-dermal border. Melanocytes form both functional and structural contacts with keratinocytes, the latter having been shown to control proliferation, differentiation and the expression of cell surface molecules on melanocytes. Several studies on melanoma metastasis and melanoma-derived experimental cell lines with different metastatic potential have shown how the alterations of the expression of the molecules involved in the regulation of motility and cellular crosstalk are one of the most important pathological events that characterize the development of melanoma tumors; in fact, the ability and the propension of transformed cells to form metastasis depend from these critical events. The list of the effectors includes cell-cell and cell adhesion molecules, matrix-degrading enzymes, cytokines and other cleavage-derived motility factors, growth factors and their receptors (81). In particular, authors have identified in the downregulation of E-cadherin and upregulation of N-cadherin adhesion proteins crucial events leading to the development of locally invasive and metastatic malignant melanoma phenotypes (82). It is actually well known that during melanoma progression the loss of E-cadherin expression disrupts normal homeostasis in the skin

by freeing melanoma cells from structural and functional regulation by keratinocytes. The loss of functional E-cadherin, paralled by a gain in N-cadherin function mediates homotypic interaction between melanoma cells, thus facilitating gap-junctional formation with fibroblasts and endothelial cells and promoting melanoma cell migration and survival. In addition, loss of E-cadherin may affect the β-catenin/wnt signaling pathways (leading to *c-myc* and cyclin D1 activation), resulting in deregulation of genes involved in growth and metastasis (82, 83). Downregulation of the original matrix receptors, such as α5β1 fibronectin-receptor, and various laminin/collagen IV receptors, such as α6β1 or α6β4, have also been found in melanoma cells (84); the altered expression of these molecules involved in the motility process and cellular crosstalk have been found to determine rapid changes in adhesion/detachment cycles of transformed cells.

Melanoma progression is further associated with activation of matrix metalloproteinases such as MMP-2 (85), and with deregulated expression of the intercellular adhesion molecules such as ICAM-1 (CD54) (86), and MCAM/MUC18 that mediates homotypic and heterotypic adhesion between melanoma cells and endothelial cells (87). Other cellular adhesion molecules of the cadherin, integrin, and immunoglobulin superfamilies are also important to both growth and metastasis of melanoma. Malignant melanoma is an excellent model for studying these molecules, due in part to a sequential series of definable stages. As the malignant phenotype of melanoma cells changes from the noninvasive radial growth phase to the vertical growth phase, which has high metastatic potential, so does the repertoire of the cellular adhesion molecules expressed on the cells surface.

CD155. Recently, a growing interest has been focused on new cellular crosstalk molecular systems, such as the lectin families. In particular, Nectin-like molecule 5 (Necl-5), also known as Polio Virus Receptor (PVR) or CD155, has come to the first line of scientific interest thanks to its multiple functions (88). As a nectin molecule, its primary function seems to be the regulation of cell-cell and cell-matrix cross talk.

Evidences support the concept that this molecule can exert a role in driving the cell motility through the matrix, and that it is basically involved in cell migration, as it has been shown how it is preferentially

localized at the leading edge of moving cells and promotes cell movement and proliferation (89). It has been shown to enhance cell movement and proliferation cooperatively with activated integrin αvβ3 and growth factors receptors, such as Platelet-Derived Growth Factor (PDGF) receptor (90). When moving cells come into contact with each other, the initial cell-cell contact that occurs via the trans-interaction of Necl-5 with Nectin-3 and integrin αvβ3 remains active. However, the trans-interaction of Necl-5 with Nectin-3 is transient. Nectins and cadherins interact with each other to form adherence junctions once Necl-5 is endocytosed, and consequently disappears from the cell surface (91). Thus, the expression of Necl-5 is downregulated when cultured cells become confluent, resulting in the suppression of cell movement and proliferation (92).

Aside with this primary function it has been outlined how Necl-5 can also function as a ligand of Natural Killer cell activating receptors DNAM-1 and CD96 (Tactile). This class of activating receptors are able to bind to molecules of the nectin famliy, like Necl-5 or Nectin 12, and mediate activatory signals to NK cells (93). Such a second function of Necl-5 is in line with the concept that its primary function is involved in eliciting cell migration and motility. NK cells, in fact, are known to be induced to attack cells with a high motility attitude, when they do not express adequate levels of MHC molecules.

Several studies have demonstrated that Necl-5 overexpression in cancer cells (both of epithelial and neurological origins, like colorectal carcinoma (94), breast carcinoma, neuroblastoma and glioblastoma (95, 96) is significant in their migration, invasion, proliferation and metastasis formation abilities (97, 98). Further studies could add knowledge on the possibilities to exploit this molecule as a target for therapeutic approaches or as a marker for cancer early detection and follow-up.

3.3 Study design

The aim of the present study was to investigate on the possible use of Necl-5 as a marker for melanoma progression, by comparing its expression levels in healthy skin samples, as well as in benign nevi and in melanoma biopsies. Cell lines have also been tested for the expression of Necl-5. Different laboratory techniques have been used.

3.4 Materials and methods

Tissue samples and patient characteristics. Archival paraffin tissue section of 91 melanocytic lesions excised between 2006 and 2010 were retrieved from the Department of Pathology at Vittorio Emanuele Hospital, Catania, Italy. The collection and storage of samples were performed according to local ethical guidelines. Institutional review board approval was obtained for this study. There were 59 CMM, including 10 melanoma in situ, 12 metastatic malignant melanoma, randomly chosen for the study (among which 8 subcutaneous melanoma lesions and 4 regional lymph node metastases), 20 BMN, 10 normal skin adjacent to different tumour masses. Clinical staging of CMM was performed on a pathological basis according to the new American Joint Committee on Cancer 2001 classification system. Diagnosis and staging of BMN had been performed on the basis of clinical, histopathologic findings. All sections of CMM were superficial spreading melanoma (SSM) and nodular melanoma (NM), at different stages (Clark's level I to III). Localization of the primary melanoma were grouped in three classes: head/neck, trunk, extremities. We stratified CMM by the Breslow tumor thickness as thin (≤1mm) and thick (>1mm). Specimens were fixed in neutral 4% buffered formaldehyde for a minimum of 24h and subsequently embedded in paraffin. The clinicopathological features of 91 melanocytic lesions are summarized in Table 5.

Cell lines and culture conditions. Human epidermal melanocyte (NHEM) cell line and melanoma cell lines (WM35, A375, M14) were

maintained in Melanocyte Growth Medium (Lonza, Walkersville, USA) and RPMI medium (Gibco, Life Technologies Inc., Milan, Italy), supplemented with 2 mmol/l L-glutamine, 100 IU penicillin and 100 μg/ml streptomycin and 2% heatinactivated fetal calf serum (Gibco Life Technologies Inc.), respectively. All cell lines were cultured at 37°C in 5% CO_2 atmosphere at constant humidity and passaged twice a week. Melanocytes and melanoma cells were grown to subconfluency, harvested and subjected to downstream analysis.

RT-PCR analysis. Total cellular RNA was extracted from cultured cell lines with *Micro-to-Midi* total RNA purification system (Invitrogen, Milano, Italy) according to the manufacturer's instructions. Reverse transcription was carried out by using *M-MLV* reverse transcriptase (Invitrogen) and random primers (Invitrogen). Semiquantitive PCR was carried out by applying standard conditions. The following primers were used (5'→3'): CD155- sense: TATCTGGCTCCGAG-TGCTTGCC; CD155 antisense ACGACGGCTGCA-AAAGTGGCG; glucose-6-phosphate dehydrogenase (G6PD) sense: ACG-TGATGCAGAACCACCTACTG; G6PD antisense: ACGACGGCTGCAAA-AGTGGCG. For quantitation, gels were scanned, and the pixel intensity for each band was determined using the *Image J* program and normalized to the amount of G6PD.

	Cases of Melanoma		Benign Nevi		χ2
	n	(%)	n	(%)	
Sex					
Male	42	(59)	14	(70)	
Female	29	(41)	6	(30)	P=0.38
Age (years)					
< 60	32	(45)	13	(65)	
> 60	39	(55)	7	(35)	P=0.1
Type of cancer					
Primary cutaneous melanoma including in situ melanoma	59	(83)			
Metastatic melanoma	12	(17)			
Type of primary melanoma					
Superficial spreading	53	(74.6)			
Nodular	18	(25.4)			
Tumor localization					
Head/neck	2	(2.8)	1	(5)	
trunk	50	(70.4)	13	(65)	P=0.8
extremities	19	(26.8)	6	(30)	
Breslow thickness					
≤1	39	(54.9)			
>1	32	(43.6)			
Clark's level					
I/II	38	(53.5)			
III	33	(46.5)			
Ulceration of primary melanoma					
Absent	55	(77.5)			
Presente	16	(22.5)			
Sentinel lymph node (SLN)					
Negative	59	(83.3)			
Positive	12	(16.7)			

Table 5. Socio-demographic and clinical features of patients with melanoma and benign nevi.

Immunoblot analysis. Immunoblot analysis was performed as described by Merrill and coworkers (99). Antibodies included anti-CD155 (ab 103630, Abcam, Cambridge, UK) and anti-β Actin (Sigma-Aldrich). CD155 antibody binding was detected by streptavidin-horseradish peroxidase complex (Roche, Indianapolis, IN) and visualized by using enhanced chemiluminescence substrate (Amersham Life Science, Piscataway, NJ, USA). β Actin was used as an internal loading control.

Flow cytometry analysis. Cell lines were washed in PBS. Cell suspensions were stained with phycoerythrin-conjugated mouse IgG1 isotype control and mouse IgG1 anti-CD155 (Bioscience, USA). Cells were analyzed by using a *FACScalibur* flow cytometer (Becton Dickinson, USA). After gating cells on a forward scatter/side scatter dot plot window on linear scale, fluorescence intensity of PE-conjugated isotype control and anti-CD155 labelled cells were analyzed in histograms on FL2 channel with logarithmic scale.

siRNA gene-expression silencing. A double stranded siRNA oligonucleotide targeting CD155 (5'-CAACUUUAAUCUGCAACGUdTdT-3') was chemical-ly synthesized (Dharmacon Research) and transfected into WM35, A375 and M14 cells using *Oligofectamine* (Invitrogen), following manufacturer's instructions by using 200 nM siRNA per 10 cm dish. Cells were incubated with siRNA in *OptiMEM* (Invitrogen) for 6 hrs after which time normal growth media was added. Cells were then incubated for 72 hours to achieve >80% knockdown of CD155. Control cells were transfected with a scrambled siRNA oligonucleotide at matching concentration. After transfection, cells were harvested and subjected to invasion assay.

Tumor invasion assay. In vitro invasion assay was done by using a cell invasion assay kit based on the manufacturer's protocol (Chemicon, Billerica, MA). Control cells and siRNA-treated cells were trypsinized and used for the invasion assay.

Immunohistochemistry. Immunohistochemical staining of NECL-5 was performed according to standard protocols by using anti-CD155 antibody (ab60115, Abcam, Cambridge, UK). Detection of primary antibody was performed by using the streptavidin–biotin–peroxidise complex system (Santa Cruz Biotechnology Inc., Santa Cruz, CA), according to manufacturer's instructions. The detection was carried out using Histostain-Plus Kit (Zymed, South San Francisco, CA). AEC (3-amino-9-ethylcarbozole) was used as a chromogen. Negative control experiments were performed as above described. Detection of YY1 was

performed by using Sigma Aldrich HPA001119 antibody, according to the manufacturer's instructions.

Image analysis. Immunolabelled and sampled tumor sections were observed using a Leica DMRB microscope (10× and 40× magnification) (Leica, Wetzlar, Germany), the images were photographed with a Canon G-9 camera (Canon, Japan) and analyzed using Image J software. Four randomly chosen fields of view were assessed in melanoma biopsies and in cell lines. A section was considered negative or positive according to the absence or presence of cytoplasmic staining. Immunoreactivity was assessed by the amount of positive malignant cells in the area. We used a staining index (SI; values 0-16) with the following formula: SI = immunostaining intensity x positive area, where intensities were scored semiquantitatively as follows: 4+ = very strong; 3+ = strong; 2+ = moderate; 1+ = weak; 0 = negative. Positive areas were defined as the epithelial area that showed positive malignant cells for NECL-5 immunoreactivity and was graded on an arbitrary scale as 0 = absent; 1+ = less than 25%; 2+ = 25% to 50%; 3+ = 51% to 75%; 4+ = more than 75%. The distribution of staining was classified as focal or diffuse. Localization of staining (membranous or cytoplasmic) was also recorded. Scoring was based upon the consensus of three histopathologists.

Gene expression datasets. Computational evaluation of NECL-5 has been performed by *Oncomine* software. Differential mRNA expression analyses among normal skin tissue versus benign melanocytic skin nevus (BMN), BMN versus cutaneous malignant melanoma (CMM) and CMM versus metastatic melanoma were explored in 3 datasets showing statistical significance less than 0.05 ($p<0.05$) (100-102). Statistical analysis was accomplished through use of ONCOMINE algorithms. Haqq Melanoma Dataset was excluded from the study as a different microarray platform has been used by the authors (103). Fold change values were considered for this analysis. Correlation between NECL-5 and Yin Yang 1 (YY1) transcript levels was analyzed according to Oncomine software in the Xu Melanoma Dataset (102).

Statistical analysis. Statistical analyses were performed using SPSS for Windows. Comparison of socio-demographic and clinical characteristics of benign nevi and melanoma patients was performed with the $\chi 2$ test. Normally distributed data were expressed as media ± SE and non normally distributed data were expressed as median (range). To correlate NECL-5 staining index and clinic-pathologic features $\chi 2$ square test was applied. Additionally, the correlations between NECL-5 expression in melanoma sections and Breslow thickness were assessed by Spearman rank correlation. For semiquantitative RT-PCR analysis, statistics was performed by using the unpaired Student's t test. The statistical differences of NECL-5 expression level between primary and metastatic melanoma samples were calculated by Student t test or one-way analysis of variance (ANOVA). Differences were considered to be statistically significant at a level of $p < 0.05$.

3.5 Results

Immunohistochemistry. Immunohistochemistry evaluation showed that NECL-5 protein is expressed in all melanoma cell lines. In detail, NECL-5 immunolabelling was mainly localized at both extracellular and intracellular level of WM35, A375 and M14 cells and a stronger immunolabelling was observed in metastatic cell lines (Figure 13).

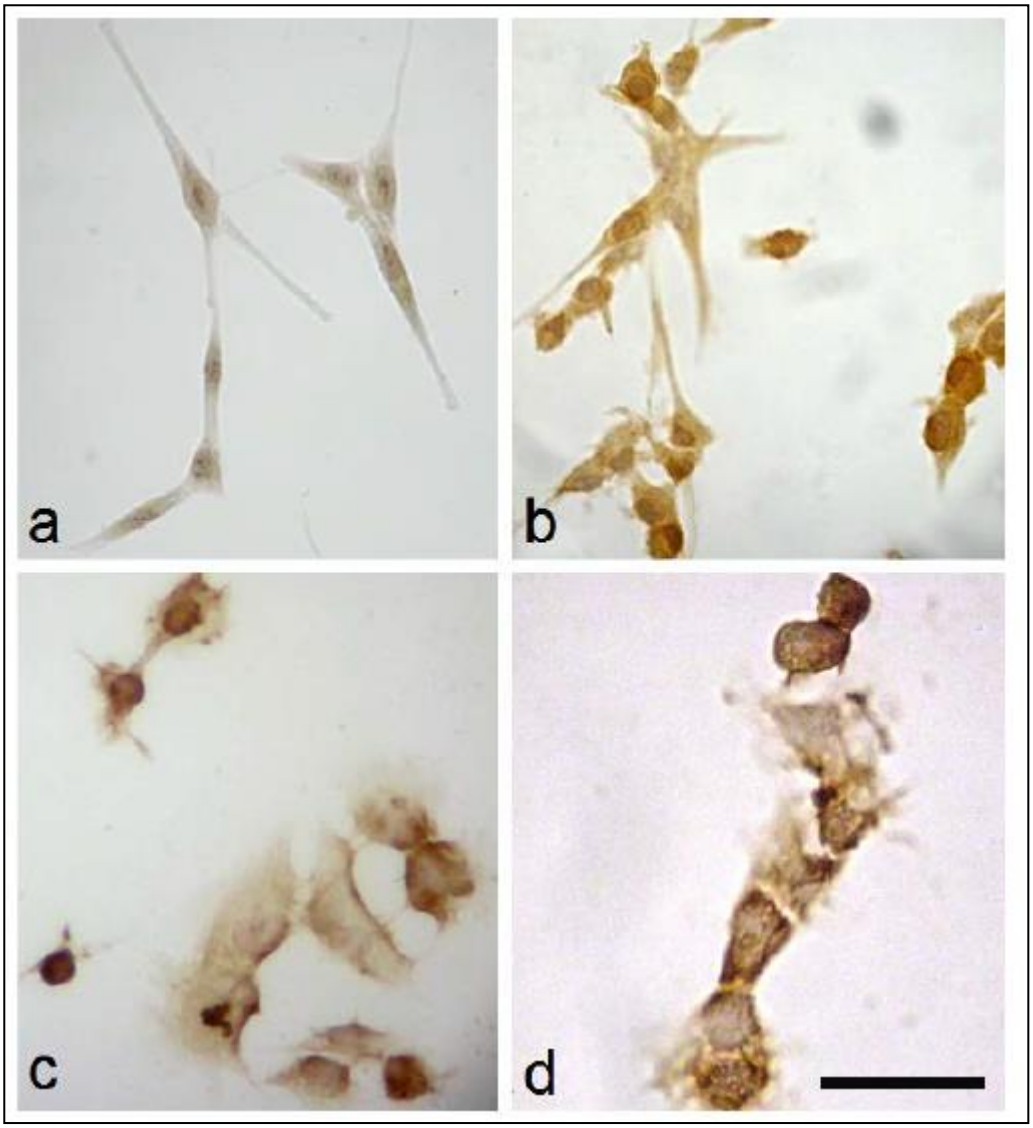

Figure 13. Immunolabelling for Necl-5 protein in normal melanocytes (NHEM) and melanoma cell lines, WM35, A375 and M14. In NHEM (a) the immunostaining is almost absent. WM35 (b), A375(c) and M14 (d) cells are labeled for Nelc-5. The protein is mainly localize at the cell membrane and at the cell leading edge (bar: 50 μm).

IHC evaluation of NECL-5 was also performed in 20 benign nevi and 71 melanoma specimens, including 12 metastatic melanoma (Figure 14). Normal skin tissues showed no immunostaining (Figure 14a) whereas a positive immunostaining was in CMMs specimens (Figure 14c and 14d). The immunopositivity for NECL-5 was also significantly different between the benign nevi (Figure 14b) and malignant lesions (primary and metastatic melanomas; Figure 14c and 14d). 10 of 20 (50%) benign nevi samples had minimal weak immunostaining of NECL-5. It was mainly detected in the outer zones of the rows of melanocytes and, almost absent, in cell-cell contacts between melanocytes (Figure 14b). In 3 nevi, NECL-5 immunostaining was present in the epidermis and upper dermis. Almost 91.5% of all melanoma specimens (primary and metastatic melanomas) showed an enhanced NECL-5 immunoreactivity (Figure 14c and 14d) when compared to NECL-5 immunoreactivity of benign nevi (14b; $p<0.0001$). In primary melanoma, NECL-5 staining was detected in cytoplasm and/or membrane of cancer cells. Immunoreactivity of NECL-5 was observed to be higher, within tumor cells, in metastatic melanomas than in primary melanoma ($p<0.001$). A strong reactivity for NECL-5 was observed in papillary dermis, and a variable reactivity in reticular dermis or around blood vessels (Figure 14d). As shown in Figure 14e and 14f, NECL-5 expression is higher in melanoma sections with thickness > 1 mm in comparison with those with thickness ≤ 1 mm.

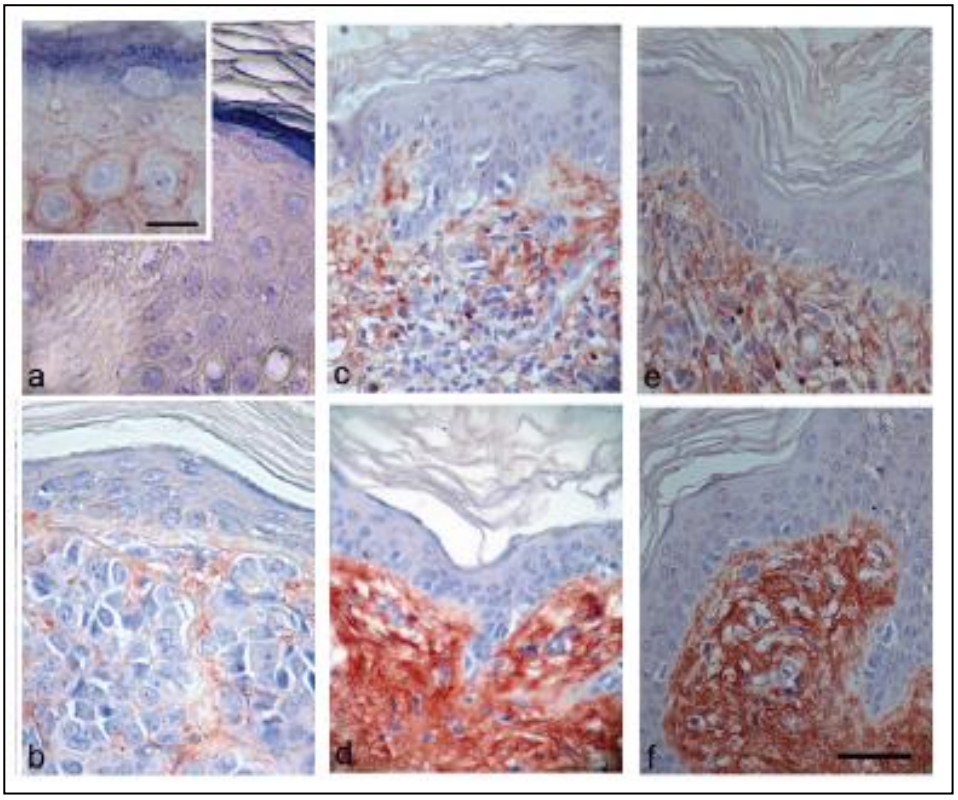

Figure 14. Representative sample of NECL-5 histological staining of skin lesions. (a) normal skin; (b) nevus; (c, d, e and f) malignant melanoma.

The immunoreactivity was represented by the assignment of staining index (SI), in which the intensity of immunostaining was multiplied by the extent of positive area in the tissue samples. The mean staining index ± SE for benign nevi was 2.3 ± 0.51; it was 7.95 ± 0.45 and 12.6 ± 1.58 for primary and metastatic melanoma samples, respectively. In this analysis, primary and metastatic melanoma showed significantly higher level of NECL-5 expression than nevi ($p<0.0001$). As shown in the Table 6, 8 of 20 (40%) benign nevi were negative, only 2 of 20 (10%) displayed moderate and 10 of 20 (50%) had weak NECL-5 staining. We found that 51% of primary melanomas samples showed strong (30 of 59 cases) or 27% moderate (16 of 59) or 12% weak (7 out of 59) immunostaining, whereas 6 of 59 (10%) were negative and those negative samples were all melanoma in situ. NECL-5 was immunohistochemically detected in all melanoma metastases. Among 12 metastasis, 8 (67%) showed strong staining, 3 of 12 (25%) moderate and 1 of 12 (8%) had weak staining intensity.

We further examined a possible correlations between NECL-5 expression profiles in melanoma samples with their clinicopathologic features. Our analysis in melanoma tissue sections revealed that NECL-5 expression was strongly correlated to lymph node involvement ($p = 0.009$) and Breslow thickness ($p = 0.004$). As expected, the comparison between the group of melanoma sections with thickness > 1 mm and those with thickness ≤ 1 mm evidenced that NECL-5 immunoreactive scores were higher in thick (score: mean 10.53 ± 0.74, $P = 0.003$) than in thin melanomas (score: mean 7.51 ± 0.59). In particular, 26 out of 32 (81.2%) thick melanoma displayed a staining of 4 +; 9.4% (3 of 32) had 3+ and 9.4% (3 of 32) showed 2+, while, 28.2% (11 of 39) thin melanoma had 4+, 25.6% (10 of 39) had 3+ and 46.1% (18 of 39) showed 2+. NECL-5 immunoscore was directly correlated to Breslow thickness ($r = 0.59$, $p = 0.0001$). These observations suggested a correlation between increased NECL-5 expression and clinical progression in melanoma. However, no evident correlations were observed between NECL-5 expression profiles and other clinicopathologic features, including age, sex, type of primary melanoma (superficial-spreading melanoma and nodular melanoma), Clark's levels and ulcerations.

Melanocytic lesions	Immunoscore			
	Strong	Moderate	Weak	Negative
Benign nevi	-	2/20 (10%)	10/20 (50%)	8/20 (40%)
Primary melanoma	30/59 (51%)	16/59 (27%)	7/59 (12%)	6/59 (10%)
Metastatic melanoma	8/12 (67%)	3/12 (25%)	1/12 (8%)	-

Table 6. NECL-5 staining intensity in melanocitic lesions.

Western blot RT-PCR. As shown in figure 15 A and B, NECL-5 expression was significantly higher in WM35, A375 and M14 cell lines compared to NHEM ($p<0.001$). Moreover, analysis with one-way ANOVA showed that NECL-5 protein levels were significantly higher in M14 and A375 cells compared to those in WM35 cells ($p= 0.002$).

Flow cytometry. Flow cytometry analysis confirmed the data of western blot and RT-PCR about NECL-5 expression in WM35, A375, M14 and NHEM cell lines (Figure 15 C).

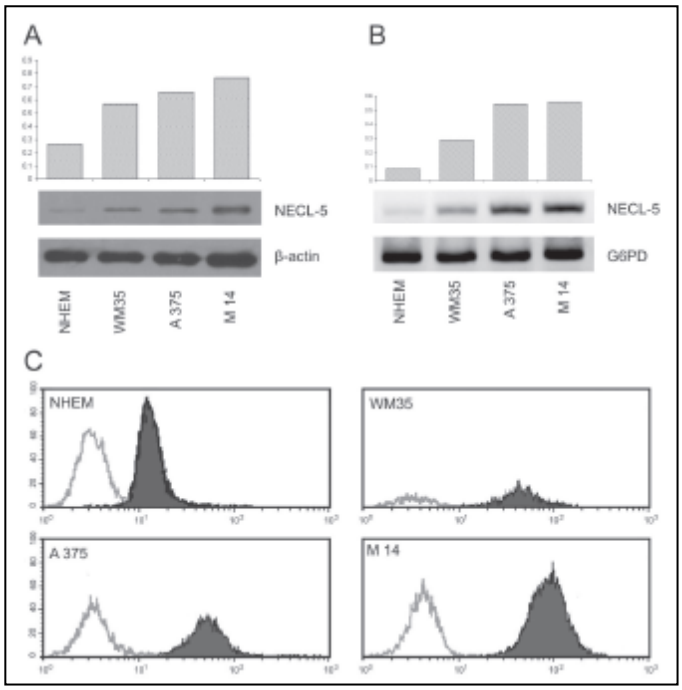

Figure 15. Protein expression analysis of NECL-5 in normal melanocytes and melanoma cell lines. (A) and (B) western blot, (C) flow cytometry.

Gene silencing and tumor invasion assay. Knockdown of NECL-5 gene in both A375 and M14 cells was used to understand the effect on cell migration. As shown in Figure 16A, the transfection of NECL-5-specific siRNAs cause an almost 70% loss of NECL-5 transcript levels compared to control both in A375 and M14 cells. A reduction of 40% of invasive capacity was observed when NECL-5 was knocked-down in melanoma cells compared with control cells ($p < 0.001$; fig. 16B).

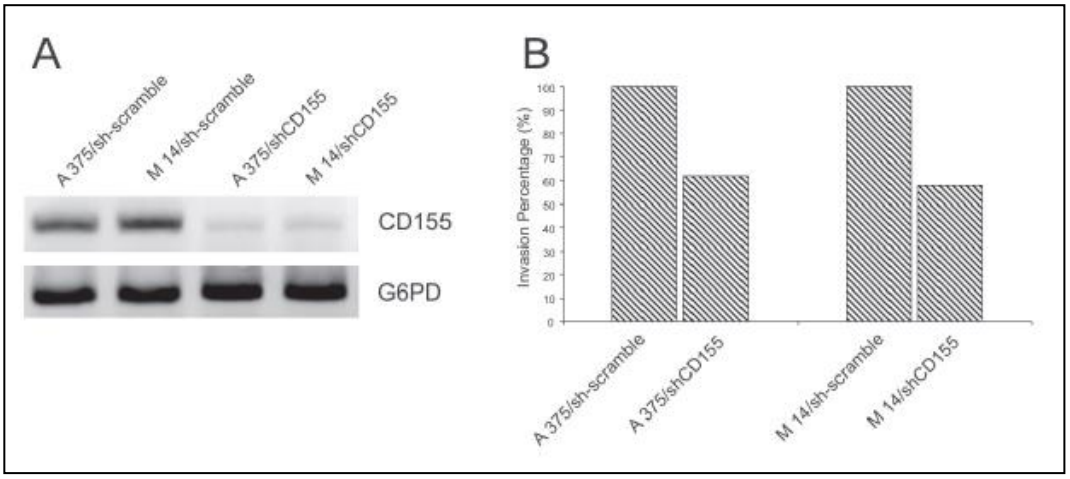

Fig 16. (A) NECL-5 expression after gene silencing. (B) Transwell migration after gene silencing.

Gene expression analysis. Transcript levels were higher in primary and in metastatic melanoma samples when compared to those of normal samples by analyzing several public available melanoma datasets.

To further confirm the association of NECL-5 with a more malignant phenotype in melanoma development, a positive correlation between NECL-5 and YY1 transcript levels has been identified by analyzing Oncomine software (r=0.468) (Figure 17). In agreement with computational identification, immunehisto-chemistry evaluation reveals that both NECL-5 and YY1 were concomitantly overexpressed in melanoma samples (Figure 18).

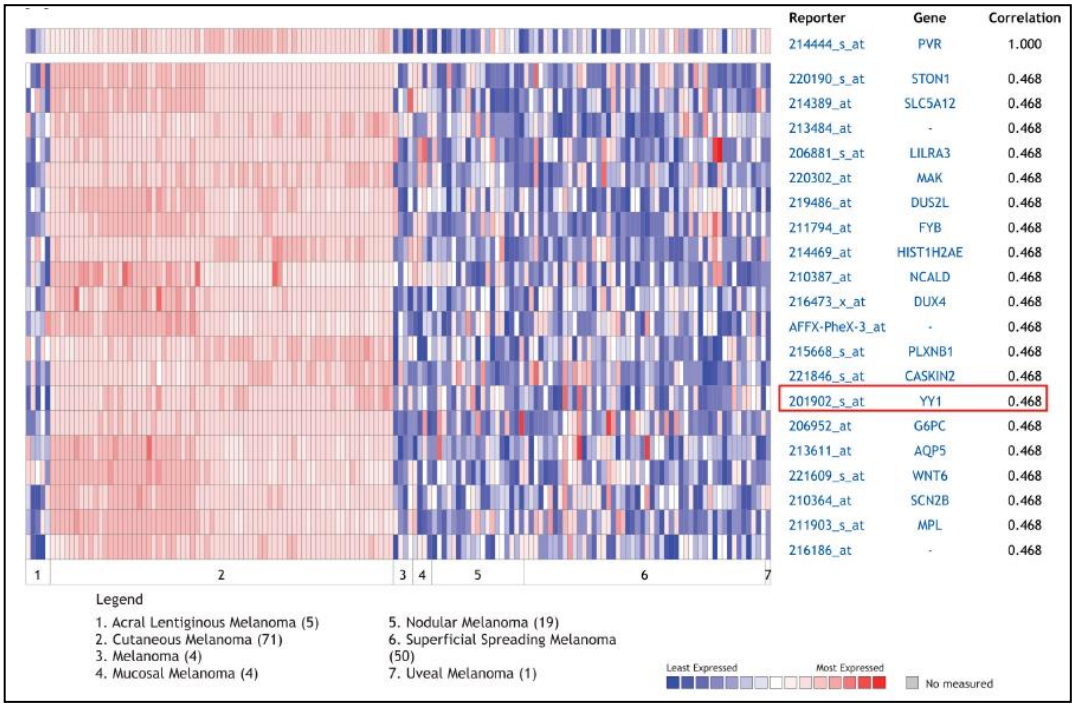

Figure 17. Correlation of YY1 with Necl-5 in melanoma datasets. Heat map of genes positively correlated with Necl-5 (r = 0,5) by Pearson correlation analysis in Xu melanoma dataset.

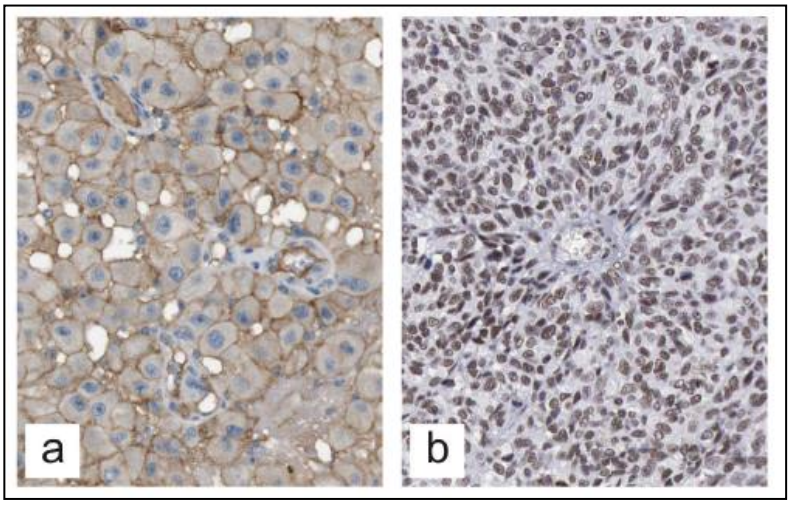

Figure 18. Necl-5 and YY1 immunohistochemistry. Immunohistochemical evaluation of Necl-5 (a) and YY1 (b) in a representative melanoma sample.

3.6 Discussion

To our knowledge, this is the first report showing the expression of NECL-5 in primary and metastatic melanoma tissues and its correlation to some clinic-pathological features by using several independent approaches. These findings suggest its role in melanoma progression. A differential expression of NECL-5 was detected between primary melanoma tissues and benign nevi. Only 60% of nevi displayed minimal or weak NECL-5 expression, whereas 91.5% of melanoma specimens showed a high NECL-5 expression. The immune-positivity for NECL-5 protein was significantly different between the benign (nevi) and malignant (in situ, invasive and metastatic melanoma) lesions; whereas it was substantially absent in normal skin. In benign nevi NECL-5 expression was mainly present in the outer zones of the rows of melanocytes and seemed to be almost absent in cell-cell interfaces between melanocytes, even if in three nevi NECL-5 immunostaining was present in the epidermis and upper dermis and declining with increasing depth. It is possible to speculate that NECL-5 expression in nevus cells enables them to invade into dermis. Benign and atypical nevi have been shown to exist in clinical and histologic contiguity with cutaneous melanoma suggesting that these melanocytic nevi are also susceptible to malignant transformation (104). These findings are consistent with other published reports describing the hypotetical role of NECL-5 overexpression in different tumors (97, 99-103). Most recently, Nakai and coworkers reported that NECL-5 expression is up-regulated in lung adenocarcinoma and has a negative effect on the prognosis of patients (105). Previously, Ochiai and others had shown that CD155 expression was up-regulated in several primary breast tumors (106). Similarly, Sloan observed that elevated espression of CD155 was detected in several primary cancer types (97). In the current study, knockdown of the gene encoding NECL-5 in A375 and M14 cells caused a reduction of nearly 40% in tumor invasion capacity and provided further data that underline the role of NECL-5 in the progression of malignant melanoma.

Our analysis in melanoma tissue specimens showed that the increase in NECL-5 immunoreactivity correlated to lymph node involvement and Breslow thickness that are considered to be major predictive factors in

melanoma microstaging (107, 108). These results seem to suggest that increased NECL-5 expression correlates to a more aggressive behaviour. In agreement with our findings, previous study showed that transformed cells gain metastatic ability owing to upregulation of NECL-5 (109, 110).

Many studies have demonstrated that overexpression of NECL-5 is implicated in the loss of contact inhibition and epithelial integrity, so to enhance cell proliferation and migration; this may in turn contribute to the dissemination of cancer cells from the original site (110). Interestingly, a novel link between NECL-5 and MMP-2 expression in glioblastoma has been demonstrated (111). MMP-2 is strongly expressed in malignant melanomas and it correlates with invasion and metastatic behavior. This could lead to speculate that the overexpression of MMP-2 and NECL-5 might be part of a unique altered regulatory program aiming to favour the loss of cell-cell adhesion molecules and then cell migration (112). Other studies have shown how some substrates of MMP-2 have been associated with cancer development and tumor progression, like E-cadherin. The loss of E-cadherin in melanocytic lesions would be found initially in nevi and more frequently in melanomas, this process appears to be one of the critical steps in the progression of melanoma (113).

Furthermore, the implication of NECL-5 in the aggressiveness of melanoma may be corroborated by its correlation to the transcription factor YY1. Recent data showed that transcript levels of the transcription factor YY1 are higher in several cancer types, including melanoma, when compared with those of normal tissue (114-117). Previous studies have observed that the inhibition of YY1 in A375 melanoma cells induces p53-mediated apoptosis after treatment with nitric-oxide donor (118). These observations have lead us to investigate whether YY1 transcript levels correlate to NECL-5 mRNA levels in melanoma. By analyzing the large series of melanoma samples in the Xu dataset, we observed that YY1 is positively correlated to NECL-5 ($r = 0.5$), providing further evidence to the idea that its overexpression is associated to a malignant phenotype in melanoma development.

3.7 Conclusions

In conclusion, we have provided evidence that NECL-5 may be an important biomarker in early diagnosis of melanoma, as it is already slightly expressed in benign nevi. Moreover, NECL-5 seems to be a sensitive indicator of melanoma progression, as it is found strongly expressed in metastatic melanoma cell lines. In primary melanoma lesions NECL-5 localization seem to suggest his possible involvement in the progression toward an invasive phenotype. Limitations of our study is the absence of clinical follow-up, including survival data. Additional studies of NECL-5 relationship with other adhesion molecules and growth factors would be useful to further address the complex processes of pathogenesis and progression in malignant melanoma. Further future goals will be to determine the molecular and cellular consequences of increased NECL-5 expression. These studies will allow the linking of NECL-5 to specific altered signaling pathways so to contribute to the development of new targeted therapeutic strategies.

3.8 References

75. Demierre MF, Sabel MS, et al: *State of the science 60th anniversary review: 60 Years of advances in cutaneous melanoma epidemiology, diagnosis, and treatment, as reported in the journal Cancer*. **Cancer**, 2008; 113 (7 Suppl): 1728-4.

76. Brenner S, and Tamir E: *Early detection of melanoma: the best strategy for a favorable prognosis*. **Clin Dermatol**, 2002; 20(3): 203-11.

77. Curtin JA, Fridlyand J, et al: *Distinct sets of genetic alterations in melanoma*. **N Engl J Med**, 2005; 353(20): 2135-47.

78. Miller AJ, and Mihm MC: Melanoma. **N Engl J Med**, 2006; 355(1): 51-65.

79. Crowson AN, Magro C, et al: *The molecular basis of melanomagenesis and the metastatic phenotype*. **Semin Oncol**, 2007; 34(6):476-90.

80. Daniotti M, Oggionni M, et al: *BRAF alterations are associated with complex mutational profiles in malignant melanoma*. **Oncogene**, 2004; 23 (35): 5968-77.

81. McGary EC, Lev DC, and Bar-Eli M: *Cellular adhesion pathways and metastatic potential of human melanoma*. **Cancer Biol Ther**, 2002; 1:459-65.

82. Hsu MY, Wheelock MJ, et al: *Shifts in cadherin profiles between human normal melanocytes and melanomas.* **J Investig Dermatol Symp Proc**, 1996; 1:188-94.

83. Hsu MY, Meier FE, et al: *E-cadherin expression in melanoma cells restores keratinocyte-mediated growth control and down-regulates expression of invasion-related adhesion receptors*. **Am J Pathol**, 2000; 156:1515-25.

84. Danen EH, Van Muijen GN, and Ruiter DJ: *Role of integrins as signal transducing cell adhesion molecules in human cutaneous melanoma*. **Cancer Surv**, 1995; 24:43-65.

85. Hofmann UB, Westphal JR, et al: *Matrix metalloproteinases in human melanoma*. **J Invest Dermatol**, 2000; 115:337-44.

86. Johnson JP: *Cell adhesion molecules in the development and progression of malignant melanoma*. **Cancer Metastasis Rev**, 1999; 18:345-57.

87. Melnikova VO and Bar-El Mi: *Transcriptional control of the melanoma malignant phenotype*. **Cancer Biology & Therapy**, 2008; 7-7:997-1003.

88. Rikitake Y, and Takai Y: *Directional cell migration regulation by small G proteins, nectin-like molecule-5, and afadin*. **Int Rev Cell Mol Biol**, 2011; 287:97-143.

89. Takai Y, Miyoshi J, et al: *Nectins and nectin‐like molecules: roles in contact inhibition of cell movement and proliferation*. **Nat Rev Mol Cell Biol**, 2008; 603-615.

90. Amano H, Ikeda W, et al: *Interaction and localization of Necl‐5 and PDGF receptor beta at the leading edges of moving NIH3T3 cells: Implications for directional cell movement*. **Genes Cells**, 2008; 13: 269‐284.

91. Irie K, Shimizu K, et al: *Roles and modes of action of nectins in cell‐cell adhesion*. **Semin Cell Dev Biol**, 2004; 15: 643‐656.

92. Ogita H and Takai Y: *Nectins and nectin‐like molecules: roles in cell adhesion, polarization, movement, and proliferation*. **IUBMB Life**, 2006; 58:334‐343, 2006.

93. Chan CJ, Andrews DM, and Smyth MJ: *Receptors that interact with nectin and nectin-like proteins in the immunosurveillance and immunotherapy of cancer*. **Curr Opin Immunol**, 2012; 24(2): 246-51.

94. Masson D, Jarry A, et al: *Overexpression of CD155 gene in human colorectal carcinoma*. **Gut**, 2001; 49: 236‐240.

95. Solecki D, Wimmer E, et al: *Identification and characterization of the cis‐acting elements of the human CD155 gene core promoter*. **J Biol Chem**, 1999; 274: 1791‐1800.

96. Solecki D, Bernhardt G, et al: *Identification of a nuclear respiratory factor‐1 binding site within the core promoter of the human polio virus receptor/CD155 gene*. **J Biol Chem**, 2000; 275: 12453‐12462.

97. Sloan KE, Eustace BK, et al: *CD155/PVR plays a key role in cell motility during tumor cell invasion and migration*. **BMC Cancer**, 2004; 4: 73.

98. Kakunaga S, Ikeda W, et al: *Enhancement of serum‐ and platelet‐derived growth factor‐induced cell proliferation by Necl‐5/Tage4/poliovirus receptor/CD155 through the Ras‐Raf‐MEK‐ERK signaling*. **J Biol Chem**, 2004; 279: 36419‐36425.

99. Merrill MK, Bernhardt G, et al: *Poliovirus receptor CD155-targeted oncolysis of glioma*. **J Neurooncol**, 2004; 6: 208-232.

100. Talantov D, Mazumder A, et al: *Novel genes associated with malignant melanoma but not benign melanocytic lesions*. **Clin Cancer Res**, 2005; 11: 7234-7242.

101. Riker AI, Enkemann SA, et al: *The gene expression profiles of primary and metastatic melanoma yields a transition point of tumor progression and metastasis*. **BMC Med Genomics**, 2008; 1:1-13.

102. Xu L, Shen SS, et al: *Gene expression changes in an animal melanoma model correlate with aggressiveness of human melanoma metastases*. **Mol Cancer Res**, 2008; 6:760-769.

103. Haqq C, Nosrati M, et al: T*he gene expression signatures of melanoma progression*. **Proc Natl Acad Sci USA**, 2005; 102:6092-6097.

104. Crowson AN, Magro CM, and Sanchez-Carpintero I: *The precursors of malignant melanoma*. **Recent Results Cancer Res**, 2002; 160:75-84.

105. Nakai R, Maniwa Y, et al: *Overexpression of NECL-5 correlates with unfavorable prognosis in patients with lung adenocarcinoma*. **Cancer Sci**, 2010; 101:1326-1330.

106. Ochiai H, Moore SA, et al: *Treatment of intracerebral neoplasia and neoplastic meningitis with regional delivery of oncolytic recombinant poliovirus*. **Clin Cancer Res**, 2004; 10:4831-4838.

107. Statius Muller MG, van Leeuwen PA, et al: *The sentinel lymph node status is an important factor for predicting clinical outcome in patients with Stage I or II cutaneous melanoma*. **Cancer**, 2001; 91:2401-2408.

108. Massi D, Borgognoni L, et al: *Thick cutaneous malignant melanoma: a reappraisal of prognostic factors*. Melanoma Res, 2000; 10:153-164.

109. Hirota T, Irie K, et al: *Transcriptional activation of the mouse NECL-5/Tage4/ PVR/CD155 gene by fibroblast growth factor or oncogenic Ras through the Raf-MEK-ERK-AP-1 pathway*. **Oncogene**, 2005; 24:2229-2235.

110. Fournier G, Garrido-Urbani S, et al: *Nectin and nectin-like molecules as markers, actors and targets in cancer*. **Med Sci**, 2010; 26:273-279.

111. Enloe BM, and Jay DG: *Inhibition of NECL-5 (CD155/PVR) reduces glioblastoma dispersal and decreases MMP-2 expression and activity*. J **Neurooncol**, 2011; 102:225-235.

112. Hanahan D, and Weinberg RA: *The hallmarks of cancer*. **Cell**, 2011; 144:646-674.

113. Danen EH, deVries TJ, et al*: E-cadherin expression in human melanoma*. **Melanoma Res**, 1996; 6:127-131.

114. *Castellano G, Torrisi E, et al: The involvement of the transcription factor YY1 in cancer development and progression*. **Cell Cycle**, 2009; 8:1367- 1372.

115. Zaravinos A, and Spandidos DA: *Yin yang 1 expression in human tumors*. **Cell Cycle**, 2010; 9:512-22.

116. Caggia S, Libra M, et al: *Modulation of YY1 and p53 expression by transforming growth factor-β3 in prostate cell lines*. **Cytokine**, 2011; 56:403-410.

117. Castellano G, Torrisi E, et al: *YY1 overexpression in diffuse large B-cell lymphoma is associated with B-cell transformation and tumor progression*. **Cell Cycle**, 2010; 9:557-563.

118. Rothweiler F, Michaelis M, et al: *Anticancer effects of the nitric oxide-modified saquinavir derivative saquinavir-NO against multidrug-resistant cancer cells*. **Neoplasia**, 2010; 12:1023-1030.

Acknowledgments

Wishing that these data can be useful for further research, special acknowledgments go to the following people and institutions whose support made the realization of these works possible:

- Prof. Maria Clorinda Mazzarino and Dr. Fabio D'amico, Department of Bio-Medical Sciences, Univeristy of Catania, Italy.

- Prof. Sergio Neri, Department of Internal Medicine, P.O. 'G. Rodolico', Azienda Ospedaliero-Universitaria 'Policlinico - Vittorio Emanuele', Catania, Italy.

- Dr. Giuseppe Astori, Dr. Elena Albiero, Dr. Katia Chieregato and Dr. Francesco Rodeghiero, Laboratory of Advanced Cellular Therapies, Department of Hematology, Ospedale 'San Bortolo' – Ulss 6, Vicenza, Italy.